

KINETICS OF LOW TEMPERATURE CO OXIDATION  
OVER ACTIVATED CARBON SUPPORTED  
Pt-CeO<sub>x</sub> CATALYST

by

Berrin Gülyüz

B. S. in Ch.E., Yıldız Technical University, 2004

Submitted to the Institute for Graduate Studies in  
Science and Engineering in partial fulfillment of  
the requirements for the degree of  
Master of Science

Graduate Program in Chemical Engineering

Boğaziçi University

2007

*to my family*

## ACKNOWLEDGEMENTS

I would like to begin by expressing my deepest gratitude to Prof. Zeynep İlsen Önsan, a person I have come to view not only as my supervisor but as my mentor. Her tutelage and guidance have been indispensable to the success of this project as well as to my education. She has been the central force behind this project providing the original motivation for this thesis. I would like to thank her for guiding me throughout my thesis. Also I would like to thank my co-supervisor Prof. Ahmet Erhan Aksoylu for providing valuable insights and for his help during any step in the experimentation and the data analysis.

I would like to express my gratitude to Prof. Ayşe Nilgün Akın, Asst. Prof. Murat Dervişoğlu and Assoc. Prof. Ramazan Yıldırım who devoted their valuable time to reading and commenting on the thesis.

I wish to thank Prof. Salih Dinçer for giving me direction and sharing his great knowledge, going back as far as my undergraduate days.

I am indebted to Fatma Soyol Baltacıoğlu for sharing all the good and bad moments with me and giving me everlasting support whenever I needed. I also want to thank Şeyma Özkara Aydınoğlu who shared her knowledge, experience and friendship with me.

Special thanks go to Feyza Gökaler, Bayram Ali Göçmen, K. Erdem Uğuz, Sadi Tezcanlı, Eyüp Şimşek, Göktaş N. Özyönüm and Tuğçe Gözaçan for giving me their support and friendship.

Cordial thanks for Bilgi Dedeoğlu, Nurettin Bektaş and Yakup Bal for their technical assistance and help.

I would like to thank my family. My father, mother and brother have all been a great source of love for me throughout the years; this thesis is primarily for them. Their

unwavering support and encouragement allowed me to pursue numerous opportunities and confront many challenges that would have seemed too difficult for me to take on alone.

Finally, I would like to thank TÜBİTAK for granting me a Master's degree scholarship which was invaluable during the course of my study. Financial support for the experimental work conducted was provided by Boğaziçi University through project DPT-03K120250 and by TÜBİTAK through project 104M163.

## ABSTRACT

### **KINETICS OF LOW TEMPERATURE CO OXIDATION OVER ACTIVATED CARBON SUPPORTED Pt-CeO<sub>x</sub> CATALYST**

Kinetics of low-temperature CO oxidation was studied both in the presence and in the absence of carbon dioxide and hydrogen over air-oxidized activated carbon supported Pt-CeO<sub>x</sub> catalyst prepared by sequential impregnation of aqueous cerium nitrate and hexachloroplatinic acid solution. Molar reactant concentrations in the feed were varied from 1 to 5 per cent CO and 1 to 2.5 per cent O<sub>2</sub> in experiments conducted in the absence of carbon dioxide and hydrogen. The effect of carbon dioxide on CO oxidation mechanism was studied by changing the carbon dioxide concentration between 2-4 per cent. In preferential CO oxidation experiments, the H<sub>2</sub> concentrations used were between 5-60 per cent. All kinetic experiments were done at 383 K and atmospheric pressure.

The experimental rate data were used to estimate the kinetic parameters of the model equations in the initial rate region for the mechanisms proposed in this study. Kinetic parameters of the reaction were calculated on the basis of simple power-law expression both in the absence and presence of CO<sub>2</sub>. The reaction orders with respect to CO, O<sub>2</sub> and CO<sub>2</sub> partial pressures were found to be -0.29, 1.07 and -1.31, respectively, in the absence of H<sub>2</sub> at 383 K. Langmuir-Hinshelwood rate expressions were also proposed for low-temperature CO oxidation in the absence of both CO<sub>2</sub> and H<sub>2</sub> and in the presence of CO<sub>2</sub>. The results show that Langmuir-Hinshelwood mechanism gives a good fit to the data in this study. However, no single rate expression can effectively describe the CO oxidation data. The effect of the presence of H<sub>2</sub> in the feed on CO oxidation rate was also investigated.

## ÖZET

### AKTİF KARBON DESTEKLİ Pt-CeO<sub>x</sub> KATALİZÖRÜ ÜZERİNDE DÜŞÜK SICAKLIK KARBON MONOKSİT OKSİDASYONU KİNETİĞİ

Sulu seryum nitrat ve heksakloroplatinik asit çözeltilerinin ardışık emdirilmesi ile hazırlanmış, hava ile yükseltgenmiş aktif karbon destekli ağırlıkça 1%Pt-1%CeO<sub>x</sub> katalizörü üzerinde düşük sıcaklık karbon monoksit oksidasyonu kinetiği karbon dioksit ve hidrojenin varlığında ve yokluğunda çalışılmıştır. Karbon dioksit ve hidrojenin yokluğunda yürütülen deneylerde, beslemedeki molar reaktant konsantrasyonları yüzde 1-5 karbon monoksit ve yüzde 1-2.5 oksijen arasında değiştirilmiştir. Karbon dioksit konsantrasyonu yüzde 2-4 arasında değiştirilerek karbon dioksitin karbon monoksit oksidasyonu mekanizmasına etkisi çalışılmıştır. Seçimli karbon monoksit oksidasyonu deneylerinde kullanılan hidrojen konsantrasyonu yüzde 5-60 arasındadır. Bütün kinetik deneyler 383 K sıcaklıkta ve atmosferik basınç altında yapılmıştır.

Deneysel verilerden elde edilen CO oksidasyonu hızları bu çalışmada önerilen mekanizmalar için model denklemlerin kinetik parametrelerinin başlangıç hız bölgesinde hesaplanmasında kullanılmıştır. Reaksiyonun kinetik parametreleri hem karbon dioksit yokluğunda, hem de varlığında basit güç yasası ifadesinin temelinde hesaplanmıştır. Hidrojenin yokluğunda, 383 K'de, karbon monoksit, oksijen ve karbon dioksit için reaksiyon mertebeleri sırasıyla -0.29, 1.07 ve -1.31 olarak bulunmuştur. Ayrıca, düşük sıcaklık karbon monoksit oksidasyonu için elde edilen deneysel veriler çerçevesinde hem karbon dioksit ve hidrojenin yokluğunda, hem de karbon dioksitin varlığında geçerli olabilecek Langmuir-Hinshelwood hız denklemleri önerilmiştir. Sonuçlar Langmuir-Hinshelwood mekanizmasının bu çalışmadaki verilere uygun olduğunu göstermektedir. Ayrıca reaktör girdisinde hidrojen bulunmasının karbon monoksit oksidasyon hızlarına etkisi de araştırılmıştır.

## TABLE OF CONTENTS

ACKNOWLEDGEMENTS.....	iv
ABSTRACT.....	vi
ÖZET.....	vii
LIST OF FIGURES.....	x
LIST OF TABLES.....	xii
LIST OF SYMBOLS/ABBREVIATIONS.....	xiv
1. INTRODUCTION.....	1
2. LITERATURE SURVEY.....	4
2.1. Fuel Cells.....	4
2.2. H <sub>2</sub> Production for Fuel Cells.....	6
2.3. Low-Temperature Removal of Carbon Monoxide.....	7
2.3.1. Low-Temperature CO Oxidation .....	7
2.3.1.1. Platinum Catalysts.....	9
2.3.1.2. Cerium Oxide Promoters.....	11
2.3.2. Low-Temperature CO Oxidation in H <sub>2</sub> -Rich Gas Streams.....	12
2.3.2.1. Platinum Catalysts.....	14
2.3.2.2. Cerium Oxide Promoters.....	15
2.4. Catalyst Supports.....	16
2.4.1. Carbon Materials as Catalyst Supports .....	18
2.5. Kinetics of CO Oxidation .....	22
2.5.1. Suggested Mechanisms and Rate Expressions for CO Oxidation...	24
3. EXPERIMENTAL WORK.....	30
3.1. Materials.....	30
3.1.1. Chemicals.....	30
3.1.2. Gases.....	30
3.2. Experimental Set-Up.....	31
3.2.1. Catalyst Preparation System.....	32
3.2.2. Microreactor Flow System.....	32
3.2.3. Product Analysis System.....	33
3.3. Catalyst Preparation.....	34

3.3.1. Pretreatment of the Activated Carbon Support.....	34
3.3.2. Impregnation Method.....	35
3.4. Kinetic Measurements.....	37
4. RESULTS AND DISCUSSION.....	40
4.1. Introduction.....	40
4.2. Kinetic Study of CO Oxidation.....	41
4.2.1. Low-Temperature CO Oxidation.....	41
4.2.1.1. Rate Calculations.....	44
4.2.2. Effects of CO <sub>2</sub> on Low-Temperature CO Oxidation.....	49
4.2.2.1. Rate Calculations.....	49
4.2.3. Effects of H <sub>2</sub> on Low-Temperature CO Oxidation.....	52
5. CONCLUSIONS AND RECOMMENDATIONS.....	57
5.1. Conclusions.....	57
5.2. Recommendations.....	58
APPENDIX A: CONVERSION VERSUS RESIDENCE TIME GRAPHS.....	59
REFERENCES.....	63

## LIST OF FIGURES

Figure 2.1.	Simplified PEM fuel cell reactions.....	5
Figure 2.2.	Schematic representation of the structure of activated carbon.....	19
Figure 3.1.	The impregnation system.....	32
Figure 3.2.	The microreactor flow and product analysis system.....	33
Figure 4.1.	Fractional CO conversion versus time for experiments 1 and 14 conducted under conditions defined in Table 4.1.....	42
Figure 4.2.	CO oxidation rate versus CO <sub>2</sub> partial pressure over 1%Pt- 1%CeO <sub>x</sub> /AC2 at 383 K using a feed composition of $P_{CO} = 0.05$ atm and $P_{O_2} = 0.025$ atm.....	51
Figure 4.3.	Effect of H <sub>2</sub> content on CO conversions over 1%Pt-1%CeO <sub>x</sub> /AC2 at 383 K.....	54
Figure 4.4.	Effect of H <sub>2</sub> partial pressure on CO oxidation rates rate.....	55
Figure A.1.	Fractional CO conversion vs. residence time graph of experiments 1-3.....	59
Figure A.2.	Fractional CO conversion vs. residence time graph of experiments 4-9.....	59
Figure A.3.	Fractional CO conversion vs. residence time graph of experiments 10-12.....	60

Figure A.4. Fractional CO conversion vs. residence time graph of experiments 13-15.....	60
Figure A.5. Fractional CO conversion vs. residence time graph of experiments 17 and 18.....	61
Figure A.6. Fractional CO conversion vs. residence time graph of experiments 19 and 20.....	61

## LIST OF TABLES

Table 2.1.	Plausible elementary reaction steps for the CO oxidation mechanism	28
Table 2.2.	Reaction orders with respect to $P_{CO}$ and $P_{O_2}$ for CO oxidation on supported and single-crystalline platinum at atmospheric pressure ...	29
Table 3.1.	Chemicals used in catalyst preparation.....	30
Table 3.2.	Applications and specifications of the gases used.....	31
Table 3.3.	Reactant and product gas analysis conditions.....	34
Table 3.4.	Reduction program for Pt-CeO <sub>x</sub> /AC2 catalyst.....	37
Table 3.5.	The reaction conditions studied over air-oxidized activated carbon supported Pt-CeO <sub>x</sub> catalyst in the absence of CO <sub>2</sub> and H <sub>2</sub> .....	38
Table 3.6.	The reaction conditions studied over air-oxidized activated carbon supported Pt-CeO <sub>x</sub> catalyst in the presence of CO <sub>2</sub> or H <sub>2</sub> .....	39
Table 4.1.	CO conversions over 1%Pt-1%CeO <sub>x</sub> /AC2 with He as balance in the absence of CO <sub>2</sub> and H <sub>2</sub> , T = 383 K.....	43
Table 4.2.	Partial pressures of CO and O <sub>2</sub> and calculated initial rates over 1%Pt-1%CeO <sub>x</sub> /AC2 in the absence of CO <sub>2</sub> and H <sub>2</sub> , T = 383 K .....	45
Table 4.3	Langmuir-Hinshelwood rate expressions tested for low-temperature CO oxidation in the absence of CO <sub>2</sub> and H <sub>2</sub> at 383 K .....	48

Table 4.4.	CO and O <sub>2</sub> conversions over 1%Pt-1%CeO <sub>x</sub> /AC2 in the presence of CO <sub>2</sub> with He as balance, T = 383 K.....	49
Table 4.5.	Effect of CO <sub>2</sub> partial pressure on CO oxidation rates over 1%Pt-1%CeO <sub>x</sub> /AC2 at T = 383 K.....	50
Table 4.6.	Langmuir-Hinshelwood rate expressions tested for low-temperature CO oxidation in the presence of CO <sub>2</sub> at 383 K.....	52
Table 4.7.	CO and O <sub>2</sub> conversions for CO oxidation over 1%Pt-1%CeO <sub>x</sub> /AC2 at 383 K in the presence of H <sub>2</sub> and balance He.....	53
Table A.1.	The calculated rate data with using the fractional CO conversion vs. residence time graphs.....	62

## LIST OF SYMBOLS/ABBREVIATIONS

$F_i$	Flow rate according to component i
$k_i^b$	Rate constant of backward reaction of step i
$k_i^f$	Rate constant of forward reaction of step i
$k_i$	Rate constant of reaction step i
$K_i$	Equilibrium constant
N	Number of experiments
p	Parameter values
$P_i$	Partial pressure of component i
$-r_i$	Reaction rate according to component i
T	Temperature
$W_{cat}$	Weight of catalyst
$x_i$	Conversion of component i
$\Delta H^\circ$	Enthalpy of the reaction at the standard conditions
$\theta_{O\bullet}$	Coverage of adsorbed oxygen on ceria sites
$\alpha$	Reaction order of carbon monoxide
$\beta$	Reaction order of oxygen
$\delta$	Reaction order of carbon dioxide
$\sigma^2$	Variance of experimental error
AC	Activated Carbon
AFC	Alkaline Fuel Cell
ATR	Autothermal Reforming
DMFC	Direct Methanol Fuel Cell
ER	Eley–Rideal
GC	Gas Chromatograph
LHHW	Langmuir-Hinshelwood-Hougen-Watson
MCFC	Molten Carbonate Fuel Cell
NMRO	Noble Metal Reducible Oxide

OSC	Oxygen Storage Capacity
PAFC	Phosphoric Acid Fuel Cell
PCFC	Protonic Ceramic Fuel Cell
PEM	Polymer Electrolyte Membrane
PEMFC	Proton Exchange Membrane Fuel Cell
PGEs	Platinum Group Elements
POX	Partial Oxidation
PROX	Preferential Oxidation
r-WGS	Reverse Water-Gas Shift Reaction
SMSI	Strong Metal-Support Interaction
SOFC	Solid Oxide Fuel Cell
SR	Steam Reforming
TOS	Time On Stream
UHV	Ultra High Vacuum
WGS	Water-Gas Shift Reaction

## 1. INTRODUCTION

Fuel cell has been receiving strong attention as an alternative power source generating electricity in a direct way for its potential higher efficiency and practically zero emissions (Caputo *et al.*, 2006). Numerous types of fuel cells have already been developed. Among them, the proton exchange membrane fuel cell (PEMFC) fuelled by hydrogen appears to be the most promising technology for vehicular applications, working at low temperature and being resistant toward the presence in the feed of reformat species, in particular CO<sub>2</sub> (Pozdnyakova *et al.*, 2006a). On the other hand, CO levels need to be decreased to values below 10 ppm as dictated by the poisoning limit of a conventional low-temperature PEM fuel cell Pt catalyst. This value may be increased to 50 ppm or higher in case Pt-Ru catalysts are applied (Kolb *et al.*, 2007).

The proton exchange membrane fuel cell is fuelled with clean CO-free hydrogen which can be produced by steam reforming (SR), autothermal reforming (ATR), or partial oxidation (POX) of natural gases, light-oil fractions and alcohols. A subsequent water-gas shift (WGS) reaction reduces the amount of CO to 0.5-1 per cent (Pozdnyakova *et al.*, 2006a). Preferential (or selective) oxidation of CO (PROX) has been recognized as one of the most straightforward and cost-effective methods for achieving acceptable CO concentrations (Arias *et al.*, 2005).

The catalytic oxidation of CO at low temperature has attracted considerable attention because of its wide applications in exhaust abatement for CO<sub>2</sub> lasers, trace CO removal in enclosed atmospheres, automotive emission control and CO preferential oxidation for proton exchange membrane fuel cells. Hence, a number of studies have been carried out with different systems for low temperature CO oxidation (Zhu *et al.*, 2005).

Much effort has been focused on the kinetics of CO oxidation. Both Eley-Rideal (gaseous CO reacting with adsorbed oxygen) and Langmuir-Hinshelwood (adsorbed CO reacting with adsorbed oxygen) mechanisms have been used, with early work favoring the Eley-Rideal (ER) mechanism. Currently, the Langmuir-Hinshelwood type is favored (Salomons *et al.*, 2007). The experimental data published and the models proposed to

correlate them have been summarized (Shalabi *et al.*, 1996). Most of the models are of the Langmuir-Hinshelwood type, and the analysis of the kinetic data indicate that the rate limiting step is the surface reaction between the adsorbed species.

In CO oxidation, platinum is arguably the most used catalyst, with palladium also being common, certainly in the works pertaining to automotive pollution control. There are a number of kinetic studies over alumina and/or ceria supported Pt and Pd catalysts under various conditions (Salomons *et al.*, 2007). On the other hand, low-temperature CO oxidation over oxidized and non-oxidized activated carbon supported Pt-SnO<sub>x</sub> catalysts has been studied in order to characterize these catalysts and to determine their activity in low-temperature CO oxidation (Aksoylu *et al.*, 2000b). Later, a range of activated carbon supported Pt-SnO<sub>x</sub> and Pt-CeO<sub>x</sub> catalysts were investigated for determining their catalytic properties and their activity for preferential CO oxidation (PROX) in hydrogen-rich streams (Özkara and Aksoylu, 2003; Şimşek, *et al.*, 2007). Although both Pt-SnO<sub>x</sub> and Pt-CeO<sub>x</sub> supported on oxidized activated carbons are found to be very efficient catalysts for selective CO oxidation, kinetic studies have not yet been reported.

The aim of this work is to bring additional insight into the kinetics of low-temperature CO oxidation over the air-oxidized activated carbon supported Pt-CeO<sub>x</sub> catalyst. Kinetic studies have been conducted in the initial rates region at a temperature of 383 K using pure and mixed feed experiments. A power function rate expression is thus established with the experimentally determined reaction orders with respect to the reactants. Effects of the presence of CO<sub>2</sub> or H<sub>2</sub> in the feed have also been investigated. Based on the correlation of steady state kinetic measurements, various Langmuir-Hinshelwood-Hougen-Watson (LHHW) type rate expressions have been tested for the preliminary modeling of low-temperature CO oxidation in the absence and presence of CO<sub>2</sub> in the feed.

Section 2 comprises a brief literature survey including information about fuel cells and H<sub>2</sub> production followed by detailed information about low temperature CO oxidation as well as preferential CO oxidation. Suggested mechanisms for CO oxidation are also summarized in Section 2. The experimental procedure followed during this study is presented in Section 3. The results obtained in the experiments and their related

discussions can be found in Section 4. Finally, the conclusions and recommendations for future work are summarized in Section 5.

## 2. LITERATURE SURVEY

### 2.1. Fuel Cells

Fuel cells for both stationary and mobile applications are being studied as a means to provide clean and economical energy (Son, 2006). They are considered to be the propulsion system of the near future, since they are more energy efficient than combustion engines and possess the necessary specific power, power density and durability to replace conventional internal combustion engines from their current applications (Avgouropoulos *et al.*, 2002).

A fuel cell is a device that converts the energy, without combustion, from a fuel (methane, propane, hydrogen) and oxygen into electricity, water and heat. There are several different types of fuel cells, each using a different chemistry and they are usually classified according to their working temperature or to the electrolyte employed. These are:

- Phosphoric acid fuel cells (PAFC)
- Proton exchange (or polymer electrolyte) membrane fuel cells (PEMFC)
- Molten carbonate fuel cells (MCFC)
- Solid oxide fuel cells (SOFC)
- Alkaline fuel cells (AFC)
- Direct methanol fuel cells (DMFC)
- Regenerative fuel cells
- Zinc air fuel cells
- Protonic ceramic fuel cells (PCFC)

Fuel cells can operate either at low or high temperature and electrolytes can be aqueous, molten and solid (Alcaide *et al.*, 2006). The alkaline, direct methanol, proton exchange membrane and phosphoric acid fuel cells operate at low temperatures. The molten carbonate and solid oxide fuel cells operate at high temperatures. Due to their durability and high power generation, phosphoric acid fuel cells, molten carbonate fuel cells and solid oxide fuel cells are being used for central power plant applications. On the

other hand, proton exchange membrane fuel cells (PEMFCs) are being used for propulsive automotive power plants (Son, 2006). Aqueous electrolytes are used in the low temperature fuel cells. Molten electrolytes are usually employed at high temperatures and the solid electrolytes (such as oxide mixtures) at quite higher temperatures (Alcaide *et al.*, 2006).

Among them, the proton-exchange membrane fuel cells (PEMFCs) possess several highly advantageous features such as a low-operating temperature, sustained operation at high current density, low weight, compactness, potential for low cost and volume, long stack life, fast start-up and suitability for discontinuous operation. These features currently make PEMFC the most promising and attractive candidate for a wide variety of power applications that range from portable/micro-power and transportation uses to large-scale stationary power for buildings and distributed generation (Wee and Lee, 2006).

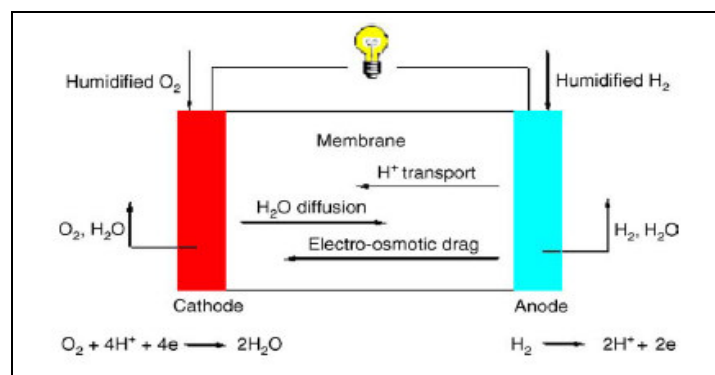


Figure 2.1. Simplified PEM fuel cell reactions (Wang, 2005)

Proton exchange membrane fuel cells work with a polymer electrolyte in the form of a thin, permeable sheet that allows hydrogen ions to pass through it. The membrane is coated on both sides with highly dispersed metal alloy particles (mostly platinum) that are active catalysts. This membrane is small and light, and it works at low temperatures (about 80°C). The electrolyte used is a solid organic polymer poly-perfluorosulfonic acid. The solid electrolyte is an advantage because it reduces corrosion and management problems.

Proton exchange membrane fuel cell performance degrades when carbon monoxide is present in the fuel gas; this is referred to as CO poisoning. It is found that CO poisons

the anode reaction through preferentially adsorbing on the platinum surface and blocking active sites, and that the CO poisoning effect is slow and reversible. There are three methods to mitigate the effect of CO poisoning: (i) the use of a platinum alloy catalyst, (ii) higher cell operating temperature and (iii) introduction of oxygen into the fuel gas flow (Baschuk and Li, 2001).

The PEMFC requires hydrogen as its fuel source since it simplifies system integration, maximizes system efficiency, and provides zero emission. However, the use of H<sub>2</sub>-PEMFCs in vehicle applications is confronted with serious problems associated with the distribution and storage of hydrogen. A promising way to overcome these problems is to produce the H<sub>2</sub> feed gas on-board using a reformer (Avgouropoulos *et al.*, 2002).

## 2.2. H<sub>2</sub> Production for Fuel Cells

Hydrogen is usually produced by autothermal reforming (ATR) of a hydrocarbon ( $\text{fuel} + \text{H}_2\text{O} \leftrightarrow \text{CO}_x + \text{H}_2$ ), where without water it is partial oxidation (POX) and without oxygen it is steam reforming (SR). It can be produced by converting a conventional fuel such as natural gas, gasoline or alcohols (methanol, ethanol) to a H<sub>2</sub>-rich gas mixture (Avgouropoulos *et al.*, 2002). In any case, hydrogen is produced together with significant amounts of CO. However, depending on the type of anode the CO concentration in the hydrogen feed must be under 1-100 ppm (Wootsch *et al.*, 2004). Because of the high sensitivity of the PEMFC anode catalysts towards even traces of CO, technologies have to be developed to decrease the CO level (Mariño *et al.*, 2004).

The water-gas shift (WGS) reaction ( $\text{CO} + \text{H}_2\text{O} \leftrightarrow \text{CO}_2 + \text{H}_2$ ) eliminates most of the CO, producing more hydrogen. This reaction is a critical step in fuel processors for preliminary CO clean up and additional hydrogen generation (Pozdnyakova *et al.*, 2006a). It is essential to adjust CO:H<sub>2</sub> ratio to the desired value (Trimm, 2005). The gas at the outlet of a reformer and water gas shift reactor typically contains 45-75 vol. per cent H<sub>2</sub>, 15-25 vol. per cent CO<sub>2</sub>, a few vol. per cent H<sub>2</sub>O, traces of unconverted fuel and, unfortunately, 0.5-1 vol. per cent CO (Sedmak *et al.*, 2003). This amount of CO is still high and needs to be removed (Pozdnyakova *et al.*, 2006a).

### 2.3. Low-Temperature Removal of Carbon Monoxide

The deep removal of CO is a critical step in PEMFC applications. In order to prevent poisoning of the fuel cell electrodes, the CO concentration needs to be reduced from ~1 per cent to below 10 ppm while conversion of H<sub>2</sub> is minimized (Ouyang and Besser, 2005). There are three techniques for carbon monoxide removal: preferential oxidation, pressure swing adsorption, methanation. CO removal by pressure swing adsorption requires expensive compressors, which cannot be applied easily in small scale systems. Methanation is a less advanced technology and becomes more complex due to the hydrogenation of CO<sub>2</sub> present in the reformat (Kolb *et al.*, 2007). Consequently, preferential oxidation of carbon monoxide appears to be the preferred solution as it is the lowest cost method without excessive hydrogen consumption and responds quickly to changes in operating conditions (Ghenciu, 2002; Trimm, 2005).

In order to achieve low CO concentration, the CO oxidation reactor is placed between the shift reactor and the fuel cell anode. Since the oxidation unit is placed between the low temperature WGS reactor at ~200°C and the PEMFC operates at ~80-100°C, the preferred temperatures for removal of CO are of the order of between those temperatures. This is important for start-up in transportation applications of fuel cells (Cheekatamarla *et al.*, 2005; Trimm and Önsan, 2001).

#### 2.3.1. Low-Temperature CO Oxidation

The oxidation of CO is a most important reaction in emission control, particularly in the clean-up of vehicle emissions (Armor, 1992).

One critical point for CO oxidation is to find a catalyst that is both highly active and highly selective towards the oxidation of carbon monoxide to carbon dioxide (Mariño *et al.*, 2004). Studies on the CO oxidation reaction have generally focused on different catalyst systems. The active components of the oxidation catalyst can be used without limitation and include base metal components, precious metal components and combinations thereof (including alloys) which are known noble metal reducible oxide (NMRO) catalysts. Base metal active components include copper, iron and cerium.

Precious metal active components include gold and platinum group metals comprising platinum, palladium, rhodium, and ruthenium (Anderson and Boudart, 1982).

The precious metals used are efficient but only start to act at about 170°C. This is true for most conventional catalysts which are not active at low temperatures and low O<sub>2</sub>/CO ratios, because O<sub>2</sub> and CO compete for the same sites. Over base-metal oxide catalysts, on the other hand, O<sub>2</sub> is held too strongly to be displaced by CO at low temperatures. Thus, an efficient low-temperature CO oxidation catalyst should accommodate both CO chemisorption and the simultaneous dissociative adsorption of O<sub>2</sub>. This has suggested the use of composite materials with different components, each having activity for one or other of these functions. Noble metal reducible oxide combinations, base metal oxides and perovskite type catalysts have been tested for their low-temperature CO oxidation performance (Trimm and Önsan, 2001).

Some combinations of a noble metal with a reducible metal oxide, an NMRO catalyst, possess a synergistic level of activity for the catalytic oxidation of CO at lower temperatures and partial pressures of O<sub>2</sub> than can be obtained by either component alone. These properties make NMRO catalysts candidates for use in CO removal from automobile emissions during cold start (Kielin, 1998). Supported noble metal catalysts, such as Au, Pt, Rh, Ru and the bimetallic Pt-Sn system, are typically used to promote the CO oxidation reaction (Pozdnyakova *et al.*, 2006a).

Low-temperature noble metal reducible oxide catalysts must exhibit strong metal-support interaction. One or more of three types of synergistic interaction between the two catalyst components may be responsible for the high efficiency observed at low temperatures (Trimm and Önsan, 2001).

- The two components may each have independent functions in the catalytic CO oxidation mechanism.
- The properties of one component may be modified by the presence of the other.
- The two components may associate at the atomic level in such a way as to form unique active sites.

In noble metal reducible oxide catalysts, neither the noble metal nor the reducible oxide alone is able to catalyze CO oxidation at temperatures below 150°C under practical conditions; hence, a synergistic interaction is present in the two-component material. The noble metal chemisorbs CO and the reducible oxide provides sites that dissociatively adsorb O<sub>2</sub>. Since CO and O<sub>2</sub> do not compete for the same adsorption sites, the inhibition of low-temperature CO oxidation by CO is eliminated (Akın *et al.*, 2001).

The above information show that catalysts containing noble metals proved to be very effective for CO oxidation at low temperatures. Among them, platinum and CeO<sub>2</sub> are two important components in the three-way catalysts for automobile exhaust purification (Zhu *et al.*, 2005).

2.3.1.1. Platinum Catalysts. Platinum group elements (PGEs) play a decisive role in the performance of exhaust systems, worldwide applied in vehicles and in some household utensils, to reduce the emission of gaseous pollutants such as carbon monoxide, nitrogen oxides and hydrocarbons (Bencs *et al.*, 2003). Pt-based and transition-metal-oxide-supported catalysts are the most promising catalysts for efficient low temperature CO oxidation with or without additional promoters. These catalysts require a mild reductive pretreatment and some H<sub>2</sub> or H<sub>2</sub>O in the feed gas to exhibit high activity (Trimm and Önsan, 2001).

One promising catalyst used for low-temperature CO oxidation is Pt/SnO<sub>2</sub>, with or without promoters (Herz *et al.*, 1993). Pt/SnO<sub>2</sub> is found to have significantly higher catalytic activity for CO oxidation at low temperatures than either Pt or SnO<sub>2</sub> alone (Boulaouache *et al.*, 1992). Pt/Al<sub>2</sub>O<sub>3</sub>, Pt/CeO<sub>2</sub> and Pt/CeO<sub>2</sub>/Al<sub>2</sub>O<sub>3</sub> are also very well known oxidation catalysts, especially used in automotive catalytic converter systems to eliminate the unburned hydrocarbons and CO (Oran and Uner, 2004).

If the low-temperature oxidation involves reaction between CO adsorbed on one component and oxygen species adsorbed on or originating from a second component, then the interface between the components will be critical. As a result, preparation techniques are expected to be, and are, vital to the preparation of active catalysts (Trimm and Önsan, 2001). Son *et al.* (2002) developed a water pretreatment method for Pt/Al<sub>2</sub>O<sub>3</sub> which

resulted in a high CO conversion at low temperatures (<100°C). The improvement was claimed to be due to the strong metal-support interaction (SMSI) between Pt and Al atoms. Serre *et al.* (1993) explored the influence of pretreatment steps of Pt-CeO<sub>2</sub>/Al<sub>2</sub>O<sub>3</sub>, with the discovery that after a reductive pretreatment, the Pt-CeO<sub>2</sub> interaction leads to a great enhancement in reactivity which was attributed to Pt<sup>0</sup>-CeO<sub>2</sub> sites localized at the platinum-ceria interface.

The past decade is characterized by numerous attempts to investigate the reaction of CO oxidation on platinum catalysts mainly at low pressures (<10<sup>-2</sup> Pa) using various physical methods. However, the literature contains an abundance of conflicting opinions both on the mechanism of CO oxidation and on the numerical values of the main kinetic parameters. It is reported by Anderson and Boudart (1982) the kinetics and mechanism of CO oxidation on Pt catalysts was studied by Langmuir and it was found that above 500 K the reaction occurs via interaction between gaseous CO molecules and atomically adsorbed oxygen. It is also reported by Anderson and Boudart (1982) that Tretyakov *et al.* cleaned the platinum surface in vacuum (10<sup>-8</sup> Pa) and studied the kinetics in a static system at low pressures. As a result of this study, it was suggested that gaseous CO reacts with oxygen whereas adsorbed CO only blocks the active sites on Pt surface.

Investigations of the interaction between chemisorbed CO and O<sub>2</sub> have shown that if the platinum surface is completely saturated with CO at low temperatures, the reaction does not occur. However, at a partly CO-free surface which provides sites for the dissociative adsorption of O<sub>2</sub>, the reaction proceeds at a high rate. Thus, on platinum, this provides evidence for the possibility of interaction between chemisorbed CO and oxygen atoms. At complete saturation of a platinum surface with atomically chemisorbed oxygen and with the addition of CO, the formation of CO<sub>2</sub> is very fast. Simultaneously chemisorption of CO also takes place. Consequently, when considering the CO oxidation mechanism it is necessary to take into account the following possible elementary steps (Anderson and Boudart, 1982; Zhdanov and Kasemo, 2003):

Reversible CO adsorption;



Dissociative O<sub>2</sub> adsorption;



Langmuir–Hinshelwood (LH) reaction between adsorbed CO and O;



Eley–Rideal (ER) reaction between gas-phase CO and adsorbed O;



Pt supported over reducible oxides ( $\text{CeO}_2$ ,  $\text{ZrO}_2$ ) presented higher activities at low temperatures than alumina and silica based catalysts due to different reaction mechanisms. For non-reducible oxides, only the metallic surface is involved in CO oxidation (a competitive Langmuir-Hinshelwood mechanism): both CO and  $\text{O}_2$  adsorb on the platinum crystallite and react together. When reducible oxides are used as support material, a non-competitive Langmuir-Hinshelwood mechanism occurs on the metal/oxide interface: CO adsorbed on the platinum surface reacts with oxygen atoms which are first dissociatively adsorbed on the support surface and then spilled over to the Pt particles (Souza *et al.*, 2006).

2.3.1.2. Cerium Oxide Promoters. Ceria is used in catalytic converters since 1980's and is an indispensable part of current catalytic converter technology. The reasons for so much attention being paid to cerium oxides are multiple: First, ceria stabilizes the metal dispersion thus favoring the amount of active surface per weight of the catalyst. Second, it promotes the water gas shift and hydrocarbon reforming reactions that play a fundamental role in the elimination of CO and hydrocarbons under reducing conditions, as well as CO oxidation under oxidizing conditions. Third and the most important reason is the oxygen storage and releasing capacity of  $\text{CeO}_2$  (Oran and Uner, 2004).

$\text{CeO}_2$  is the oxide of the rare-earth metal cerium, which may exist in several compositions due to the capacity of Ce to switch between the two oxidation states of  $\text{Ce}^{3+}$  and  $\text{Ce}^{4+}$  (Luengnaruemitchaia *et al.*, 2004). From a more general standpoint,  $\text{CeO}_2$  is active in transient oxygen storage, and as a catalyst support, it can promote oxidation even under oxygen-poor conditions. Ceria-supported platinum, rhodium, and palladium catalysts are also remarkably active in the low-temperature oxidation of CO, and they are able to

oxidize carbon monoxide even in the absence of oxygen, in the so-called “oxygen storage capacity” (OSC) measurement. Both Pt and Pd on ceria are also active in CO oxidation (without hydrogen), whereas Pd is poorly active in the presence of hydrogen (Pozdnyakova *et al.*, 2006a).

The change in the activity of the noble metal catalyst towards the CO oxidation reaction in the presence of CeO<sub>2</sub> is attributed to the change in the reaction mechanism. Each of the mechanistic steps, adsorption and desorption of the reactants, surface reaction and desorption of products of CO oxidation has been probed extensively with surface science techniques, as has the interaction between adsorbed O atoms and CO molecules over supported platinum, rhodium and palladium catalysts. Although the oxidation of CO over supported platinum, rhodium and palladium catalysts has been the subject of numerous studies, there is little agreement on reaction orders in literature (Oran and Uner, 2004).

Ceria enhances the reactivity of Pt when it is prereduced. The presence of ceria together with Pt seems to lead to new very reactive sites on Pt-CeO<sub>2</sub>/Al<sub>2</sub>O<sub>3</sub>. The reaction on Pt-CeO<sub>2</sub>/Al<sub>2</sub>O<sub>3</sub> may consist of the formation of CO<sub>2</sub> via the reduction of the interfacial ceria by CO adsorbed on Pt and a noncompetitive Langmuir–Hinshelwood mechanism can be imagined on the metal/oxide interface. The CO<sub>2</sub> desorption leads to vacant sites on the interfacial Pt and makes the dissociative adsorption of gaseous oxygen possible. Ceria is then regenerated by a spillover phenomenon of O<sub>ads</sub> (on the Pt sites of the Pt-CeO<sub>2</sub> interface) toward Ce<sub>2</sub>O<sub>3</sub> and reoxidation of the interface into CeO<sub>2</sub>. This interpretation is described by three consecutive steps as shown below (Serre *et al.*, 1993).

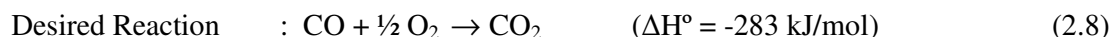


### 2.3.2. Low Temperature CO Oxidation in H<sub>2</sub>-Rich Gas Streams

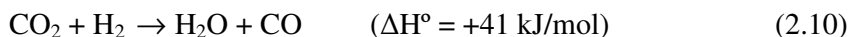
Considering the problems associated with other methods for CO removal, the selective catalytic oxidation of CO which has to be achieved in the presence of CO<sub>2</sub> and

H<sub>2</sub>O with minimum H<sub>2</sub> oxidation, seems to be the most straightforward and efficient method to reduce the residual CO in the reformat to desired levels (~10 ppm). Any remaining CO is reduced to ppm levels by preferential oxidation reaction which is the selective catalytic oxidation of CO in the H<sub>2</sub>-rich reformat using O<sub>2</sub> (Cheekatamarla *et al.*, 2005). It consists of a catalytic process aiming to selectively convert CO to CO<sub>2</sub> with air injection in the presence of large amounts of H<sub>2</sub> (around 50 vol. per cent) that must be oxidized in as much as possible limited amounts (Caputo *et al.*, 2006).

In the preferential CO oxidation reaction system, the following two oxidation reactions occur (Choi and Stenger, 2004).



In an oxygen deficient atmosphere in a PROX reactor, carbon monoxide can be formed again by the reverse water–gas shift reaction (r-WGS) (Kolb *et al.*, 2007):



Preferential oxidation of CO is rapid and responds quickly to changes in operating conditions, but it is essential to choose catalysts and operating conditions that minimize the oxidation of hydrogen (Trimm, 2005). Three obvious possibilities can be considered. It may be possible to find a catalyst that adsorbs CO but not H<sub>2</sub>, and hence favors selective oxidation of CO. It may be possible to operate at a temperature where CO is oxidized and H<sub>2</sub> is not. Finally, it may be possible to find a catalyst where both CO and H<sub>2</sub> are oxidized, but kinetic parameters lead to preferential CO oxidation at the cost of only small amounts of H<sub>2</sub> oxidation (Trimm and Önsan, 2001).

Catalysts identified as suitable for low-temperature CO oxidation are also possible candidates for the selective oxidation.

2.3.2.1. Platinum Catalysts. Pt/Al<sub>2</sub>O<sub>3</sub> has been the most studied PROX catalyst because of its high CO conversion and stability at moderate temperatures (~200°C). With this system, Kahlich *et al.* (1997) observed a maximum CO conversion at 200°C with a selectivity of ~40 per cent. They found that H<sub>2</sub> with surface oxygen can produce a hydroxyl intermediate which enhances the catalytic activity at temperatures below 200°C. Using the same catalyst system, Zafiris and Gorte (1993) discovered a relationship between CO desorption and Pt particle size, i.e., the CO desorption rate rises with the decreasing Pt particle size at a given loading, which in turn influences the CO reaction rate. In order to improve the PROX reaction activity at lower temperature (~100°C), Roberts *et al.* (2003) explored Pt/Al<sub>2</sub>O<sub>3</sub> promoted with Fe, which provides independent O<sub>2</sub> adsorption sites when Pt sites are dominated by adsorbed CO at low temperatures and hence increases the CO oxidation activity.

Korotkikh and Farrauto (2000) investigated the selective oxidation of CO over Pt/alumina and found that metal oxide promoters enhanced the activity of the catalysts even at low temperatures. Igarashi *et al.* (1997) investigated Pt supported zeolites. Their results showed that the selectivity was affected by supports and Pt/mordenite showed the highest conversion of CO to CO<sub>2</sub>. They also found that 1 per cent CO in the gas feed was never completely oxidized on Pt/Al<sub>2</sub>O<sub>3</sub> catalyst even though the O<sub>2</sub> amount added into the inlet gas was high (~3 per cent). Manasilp and Gulari (2002) showed that a 2 per cent Pt/alumina sol-gel catalyst in a stream of mostly hydrogen with oxygen can clean CO down to a few ppm.

These results show that the selectivity for CO oxidation, compared to H<sub>2</sub> oxidation, on alumina supported catalysts can be improved at low oxygen concentrations if the oxygen supply to Pt is increased. In automotive three-way catalysts, the activity of Pt catalysts can be improved through O<sub>2</sub> storage components like CeO<sub>2</sub> as also mentioned in Section 2.3.1.2.

The detailed mechanism of the simultaneous oxidation of CO and H<sub>2</sub> over noble metals is not yet fully understood. H<sub>2</sub> oxidation is strongly inhibited by the presence of CO, because CO chemisorption on noble metal surfaces is much stronger than H<sub>2</sub> or O<sub>2</sub> chemisorption (Trimm and Önsan, 2001). Consequently, CO blankets the metal surface,

displacing the weakly chemisorbed  $H_2$  and  $O_2$  species, and prevents reaction unless the temperature is high enough to desorb some of the CO on the surface. This indicates that the light-off behavior of noble metals in CO– $H_2$ – $O_2$  mixtures is dominated by the kinetics of CO oxidation rather than by the kinetics of  $H_2$  oxidation (Oh and Sinkevitch, 1993). Alternatively, the  $H_2$  in the feed can interact with CO chemisorbed on the surface to form a complex such as H–CO; its easier desorption from the surface may increase the CO oxidation activity significantly (Trimm and Önsan, 2001).

Pt itself is active both in hydrogen and CO oxidation, and an obvious reaction route is that products of these reactions,  $CO_2$  and  $H_2O$ , desorb from Pt. The selectivity is determined only by the competitive adsorption of CO,  $H_2$ , and  $O_2$ . Hydrogen adsorption on Pt (and hence the possibility toward nonselective oxidation), is strongly suppressed by the high (but not total) CO coverage, even in excess  $H_2$  for the Pt/ $Al_2O_3$  system. Nevertheless, Pt/ $CeO_2$  behaves differently than Pt/ $Al_2O_3$  in the PROX reaction (Pozdnyakova *et al.*, 2006a).

2.3.2.2. Cerium Oxide Promoters. Ceria can be an adequate support for Pt when one has to lower the CO concentration in a hydrogen-rich stream by using the PROX reaction at low temperature and/or with a minimum hydrogen loss. Unfortunately, ceria-supported platinum was found to be too active in hydrogen oxidation as well, and cannot be considered as an effective PROX catalyst above 130°C. Nevertheless, ceria can be considered as a beneficial additive to supported Pt catalysts (Özkara and Aksoylu, 2003; Wootsch *et al.*, 2004).

Noble metals dispersed on ceria containing oxide supports represent a special class of supported catalysts for PROX. Their particular behavior was demonstrated in various reactions, mainly in oxidations but also in reaction of hydrocarbons under reducing environments. The irregular properties of noble metal-ceria systems were attributed to the reducibility of the ceria support, which (i) can supply extra oxygen to the metallic site by a back spillover process, (ii) may cause increased hydrogen spillover when it is present in the reaction mixture and (iii) induce electronic and/or structural changes of metal particles by strong metal-support interaction (Teschner *et al.*, 2006).

Son (2006) indicated that adding Ce to Pt/ $\gamma$ -Al<sub>2</sub>O<sub>3</sub> produces higher CO conversion and selectivity at lower temperatures and lower O<sub>2</sub> to CO ratios because of an enhanced oxygen supply to the Pt. It was proposed that ceria-based supported platinum or iridium catalysts were shown to be suitable for the removal of CO in the presence of large quantities of hydrogen via the preferential oxidation of CO (Mariño *et al.*, 2004).

Kolb *et al.* (2007) proposed that the promotion of Pt/TiO<sub>2</sub> catalysts with ceria provides sites that enhance CO conversion and selectivity at low temperature. They found that Pt-CeO<sub>2</sub>/TiO<sub>2</sub> catalyst shows high activity and selectivity below 100°C, whereas the unpromoted Pt/Al<sub>2</sub>O<sub>3</sub> appears to be the best catalyst at 100°C and higher temperatures.

Mariño *et al.* (2004) proposed that the preferential oxidation of CO over ceria-supported catalysts could occur via a non-competitive Langmuir-Hinshelwood mechanism. Such a mechanism should involve the reaction between the CO adsorbed on the noble metal (Pt or Ir) particles and the oxygen atoms previously activated on the support.

## 2.4. Catalyst Supports

A support can be described as an inert substance that provides a means of spreading out an expensive catalyst ingredient such as platinum for its most effective use, or a means of improving the mechanical strength of an inherently weak (metal/active phase) catalyst (Satterfield, 1991).

The support chosen for a catalyst has a critical impact on catalyst activity, selectivity and ease of catalyst recycling. The support can impart an acidic or basic environment for the active catalyst component. Each support chemistry has different tendencies towards impurities (which can poison the desired reaction or enhance a competing reaction). In addition, each support chemistry has a unique range of available pore size distributions and stability to thermal, hydrothermal or acidic conditions. The selection of a support is based on its desirable characteristics such as the following (Satterfield, 1991):

- A support must have desirable mechanical properties including attrition resistance, hardness, and comparative strength.

- It should be stable under reaction and regeneration conditions.
- It should provide enough surface area to guarantee targeted dispersion of active phases. High surface area is usually, but not always, desirable.
- The support must supply porosity, including average pore size and pore-size distribution. High area implies fine pores, but relatively small pores may become plugged in catalyst preparation, especially if high loadings are sought.
- It should have low cost.
- It should either be inert or provide active sites for activity or strong metal/support interaction depending on the reaction.

A supported catalyst facilitates the flow of gases through the reactor and the diffusion of reactants through the pores to the active phase, improving the dissipation of reaction heat, retarding the sintering of the active phase or increasing the poison resistance (Rodriguez-Reinoso, 1998). Some supports that are widely used in industry are as follows:

- Alumina: They have a wide range of surface areas and pore volumes. The supports can be treated for excellent stability at high temperatures to avoid agglomeration/sintering of surface metals.
- Carbon Hybrids: They are a new class of catalyst supports that combine the features of carbon and solid oxide supports to provide catalytic surfaces with unique properties.
- Clay: These supports are inexpensive and can provide some catalytic functionality at higher temperatures.
- Silica: They are designed to have the broadest range of surface areas and pore volumes. Silica can be surface-treated to minimize additional catalytic effects. These materials can be used over a wide range of pH conditions.
- Zeolite: They are designed for reactions that can take advantage of the shape-selectivity or size exclusion of the zeolite pores.

The use of carbonaceous materials, especially activated carbon, as catalyst supports also continues to increase because of the great versatility of these materials (Fuente *et al.*, 2001).

### 2.4.1. Carbon Materials as Catalyst Supports

Carbon materials have been used for a long time in heterogeneous catalysis, because they can act as direct catalysts or, more important, they can satisfy most of the desirable properties required from a suitable support (Rodriguez-Reinoso, 1998).

Compared with oxide supports, carbon materials have considerable advantages such as (Aksoylu *et al.*, 2001):

- a high specific surface area up to 3000 m<sup>2</sup>/g,
- high stability in acidic and basic media,
- easy modification of textural properties and surface chemical properties, and
- easy recovery of precious metals supported on carbon materials.

Moreover, the varieties of available forms (e.g. graphite, carbon black, activated carbon, activated carbon fibers, carbon nanotubes and carbon molecular sieves) make carbon materials very attractive as catalysts or supports for metal catalysts (Chen *et al.*, 2006). Among them, activated carbon and carbon black are the carbon materials of choice for most carbon-supported catalysts (Rodriguez-Reinoso, 1998).

Activated carbon products can be characterized by their physical properties and activity characteristics. Important physical properties of activated carbon are surface area, product density, mesh size, abrasion resistance and ash content. High surface area and a well developed porosity are essential for achieving large metal dispersions, which usually results in a high catalytic activity. If, on the other hand, the addition of a promoter is essential for the catalyst, the presence of a high surface area is very important. The surface area and porosity available in activated carbon are usually much larger than those available in alumina or silica, although it is also true that a very large proportion of the surface area is contained within micropores (Fraga *et al.*, 2002; Rodriguez-Reinoso, 1998).

All activated carbons have a porous structure, usually with a relatively small amount of chemically bonded heteroatoms (mainly oxygen and hydrogen). In addition, activated carbon may contain up to 15 per cent of mineral matter (the nature and amount is a

function of the precursor), which is usually given as ash content. It is generally accepted that the average structure (Figure 2.2) consists of aromatic sheets and strips, often bent and resembling a mixture of wood shavings and crumpled paper, with variable gaps of molecular dimensions between them, these being the micropores (Rodriguez-Reinoso, 1998).

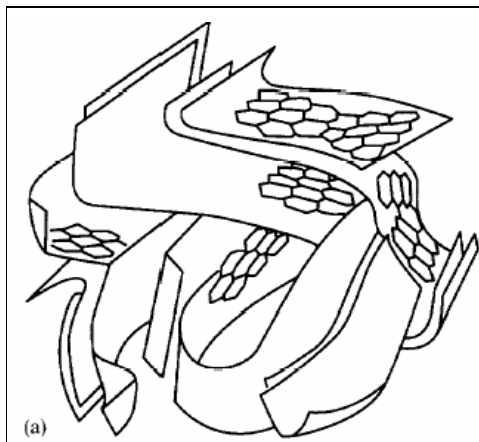


Figure 2.2. Schematic representation of the structure of activated carbon (Rodriguez-Reinoso, 1998)

The excellent adsorption properties of activated carbons are essentially attributed to their large surface area, high degree of surface reactivity, and vast infrastructure of pores and micropores, which makes the internal surface accessible, enhances the adsorption rate and increases the saturation capacity. Although most of the adsorption takes place in the micropores of activated carbon, mesopores and macropores play very important roles in any adsorption process, because they serve as a passage for the adsorbate to the micropores, since only a few of these are placed in the outer surface of the carbon particle (Rodriguez-Reinoso, 1998). Maruyama and Abe (2005) indicated that the high surface area of activated carbon is advantageous for Pt dispersion, since it was shown that the specific surface area of the dispersed Pt increases in accordance with that of the carbon black support.

The above information shows that the carbon structure offers an unparalleled flexibility for tailoring catalyst properties to specific needs, and this flexibility is a

consequence of a porous structure which determines the active phase loading, a chemical structure which influences the interaction with molecules of different nature and a wide range of active sites. In this respect, a summary of the virtues of carbon surfaces would be convenient (Rodriguez-Reinoso, 1998):

- The carbon structure is resistant to acidic or basic media,
- The structure is stable at high temperatures (even above 1000 K),
- The pore structure (constituted by slit-shaped pores, something very important when shape selectivity is a must in catalysis) may be tailored to obtain the pore size distribution needed for a given reaction,
- Porous carbons can be prepared with different physical forms (granules, pellets, extrudates, cloth, fibers, etc.),
- Although carbon is usually hydrophobic, the chemical nature of the surface can be modified to increase the hydrophilicity, and even carbons with ion-exchange properties can be prepared,
- The active phase can be easily recovered from spent catalysts by burning away the carbon support (very important when the active phase is a precious metal), and
- The cost of carbon supports is usually lower than conventional supports such as alumina and silica.

Although, carbon is considered to be an inert material in comparison with other catalyst supports, its surface is not as inert as expected due to the formation of active sites by the presence of heteroatoms (O, H and N). In terms of catalyst preparation, the presence of oxygen bearing groups is of great interest. Most of the chemical properties of activated carbon come from the incorporation of oxygen during its production, forming oxides, i.e. carboxylic, phenolic, lactonic and etheric groups which are responsible both for the acid/base and the redox properties of activated carbons. In the literature, it has been proposed that the surface chemistry of the support determines the precursor/support interaction and hence the reducibility of the species formed (Aksoylu *et al.*, 2000a).

It has been well established in the literature that the surface oxygen groups, which form anchoring sites for metallic precursors as well as for metals, dominantly determine the properties of activated carbon as a catalyst support material. The acidic groups on the

surface decrease the hydrophobicity of the carbon, leading to the accessibility of the surface to aqueous metal precursors, while the less acidic groups increase the interaction of the metal precursor or the metal particle with the support and, as a consequence, minimize the sintering propensity of metal on carbon (Aksoylu *et al.*, 2001).

It is well known that the interaction of the active phase with the support can be modified by pretreatment of the support. The catalytic behavior of activated carbon-supported noble metal catalysts can be modified by oxidation treatments of the support prior to metal loading. Different oxidizing treatments, both in the gas and in the liquid phase, can be used to perform chemical surface modifications of activated carbons (Fraga *et al.*, 2002). The main goal of oxidation is to obtain a more hydrophilic surface with a relatively large number of oxygen-containing surface groups (Aksoylu *et al.*, 2000a).

It has been proposed that the oxidation treatment changes the textural and surface chemical properties of the activated carbon: a well-suited material for catalyst applications can be obtained by air oxidation, leading to high mesoporous surface area and micropore volume, and to a weakly acidic surface (Aksoylu *et al.*, 2003).

In spite of the unique properties mentioned, activated carbon has a main disadvantage as a catalyst support: it can not be used in gas phase oxidation above 500 K. Keeping in mind the beneficial effects of the modifications via support pre-treatments, preparation methods and metal ratios on the catalytic properties, as well as the temperature limit in oxidation reactions, the use of activated carbon supported catalysts might be adequate for the low-temperature CO oxidation (Aksoylu *et al.*, 2000b). In the literature, studies on CO oxidation both in the absence and in the presence of H<sub>2</sub> (preferential oxidation) over activated carbon supported catalysts were reported.

Aksoylu *et al.* (2000b) studied CO oxidation activities of Pt-SnO<sub>x</sub> catalysts supported on un-oxidized and oxidized activated carbon in the absence of H<sub>2</sub> and reported that the HNO<sub>3</sub>-oxidized activated carbon supported Pt-SnO<sub>x</sub> prepared by sequential impregnation showed the highest activity.

In a later study, it was demonstrated that activated carbon is indeed a promising candidate as a catalyst support for selective CO oxidation in H<sub>2</sub>-rich streams over Pt-SnO<sub>x</sub> and Pt-CeO<sub>x</sub> catalysts and that the oxygen bearing surface groups of activated carbon lead to enhanced Pt-SnO<sub>x</sub> or Pt-CeO<sub>x</sub> interaction, and alloy formation in the case of Pt-SnO<sub>x</sub> (Özkara and Aksoylu, 2003).

Şimşek *et al.* (2007) investigated the effects of the presence of CO<sub>2</sub> and (CO<sub>2</sub>+H<sub>2</sub>O) in the feed on the performances of the HNO<sub>3</sub>-oxidized activated carbon supported Pt-SnO<sub>x</sub> and air-oxidized activated carbon supported Pt-CeO<sub>x</sub> catalysts that have been previously tested for CO oxidation in a dry, CO<sub>2</sub>-free and H<sub>2</sub>-rich feed stream by Özkara and Aksoylu (2003). They indicated that the conversions of CO over air-oxidized activated carbon supported Pt-CeO<sub>x</sub> increase from 20 to 100 per cent with the addition of CO<sub>2</sub> and (CO<sub>2</sub>+H<sub>2</sub>O).

The higher CO conversions obtained in the presence of CO<sub>2</sub> over catalysts with oxidized activated carbon supports can be attributed to their unique properties; oxidative pretreatments enhance the construction of surface oxygen bearing groups that provide anchoring sites for metallic precursors as well as for metals and thus increase the dispersion of Pt metallic crystallites on activated carbon supports (Aksoylu *et al.*, 2001).

## 2.5. Kinetics of CO Oxidation

Low-temperature oxidation of carbon monoxide is an important reaction in environmental catalysis, the challenge being to lower significantly the light off temperature of the catalysts. Many research groups have been looking for new catalysts or investigating the mechanism of the reaction. The supported catalysts used for low-temperature CO oxidation are quite complex; thus, determining how they function has been difficult, even though CO oxidation is a relatively simple catalytic reaction (Oh and Hoflund, 2007).

Catalysts break forces which inhibit the reaction of molecules and provide increasing reaction rates involving adsorption-desorption. If the reaction is structure sensitive, the activity and selectivity are dependent on the particle sizes or surface-active sites. Therefore, the reaction kinetics, usually described by the well-known Langmuir-

Hinshelwood (LH) models, must take in account the transient behavior of the surface during the reaction itself, modifying the sites and the adsorption-desorption phenomena and consequently the reaction mechanism. Therefore, the true kinetics is obtainable after surface characterization with reactions (Schmal *et al.*, 2005).

Kahlich *et al.*, (1997) reported that in early reviews by Engel and Ertl, focusing on the CO oxidation reaction on both single crystals and polycrystalline materials under UHV (ultra high vacuum) conditions, a distinction was made between two reaction regimes:

- a high rate branch where the CO surface concentration is very small, occurring at high temperatures and/or  $\lambda$  values (oxidizing conditions),
- a low rate branch in which the surface is predominantly covered with adsorbed CO, occurring at low temperatures and/or  $\lambda$  values (reducing conditions),

where  $\lambda$  is the process parameter that is defined as:

$$\lambda = \frac{2P_{O_2}}{P_{CO}} \quad (2.11)$$

Langmuir-Hinshelwood mechanism was proposed for both cases. The low rate branch is associated with a reaction order approaching -1 for  $P_{CO}$  and close to +1 for  $P_{O_2}$  (CO desorption limited), while the high rate branch exhibits a reaction order of +1 for  $P_{CO}$  and zero for  $P_{O_2}$ . More recent studies dealing with high-pressure CO oxidation on single-crystalline platinum metals and supported Pt-catalysts come to similar conclusions, indicating that the reaction mechanism of CO oxidation under UHV and high pressure conditions are essentially identical (in the absence of mass transport effects) (Kahlich *et al.*, 1997).

Assuming that the addition of H<sub>2</sub> to the CO/O<sub>2</sub> mixture does not fundamentally alter the CO oxidation mechanism, one would expect the reaction to occur in the low rate branch, i.e., on a surface predominantly covered with adsorbed CO (CO<sub>ads</sub>) at conditions

which prevail in the PROX process on Pt/  $\gamma$ -Al<sub>2</sub>O<sub>3</sub>, i.e., at temperatures below 250 °C and  $\lambda \leq 2$ , where  $\lambda$  is shown in Equation (2.10) (Kahlich *et al.*, 1997).

Grass and Lintz (1997) studied the kinetics of CO oxidation by oxygen in the 0–80°C temperature interval on Al<sub>2</sub>O<sub>3</sub>-supported Pt/SnO<sub>2</sub> catalysts. The results of rate measurements and titration experiments indicated that the chemisorption of CO is restricted to Pt, whereas oxygen is adsorbed both on Pt and SnO<sub>2</sub>. At low CO concentrations, the reaction was first order in CO, whereas at high CO and O<sub>2</sub> concentrations, it is zero order in both CO and O<sub>2</sub>. The sharp decrease between the two domains is typical and was explained by the transition from an oxygen-covered surface to a CO-covered one (Trimm and Önsan, 2001).

In the PROX reaction on ceria-supported Pt, a noncompetitive Langmuir–Hinshelwood mechanism has been described, involving CO activation on Pt particles and their reaction with oxygen activated from the support on the metal/oxide interface at low temperatures (T = 363–423 K). Both competitive and noncompetitive reaction pathways, as well as reaction on the ceria support, have been proposed for higher temperatures (Pozdnyakova *et al.*, 2006a).

### 2.5.1. Suggested Mechanisms and Rate Expressions for CO Oxidation

Catalysis and kinetics have made major contributions to many areas of chemical industry and are still very important in homogeneous and heterogeneous reactions (Fogler, 1999). The main questions arising from the scientific point of view are the understanding of the reaction mechanism and the kinetics of CO oxidation (Schmal *et al.*, 2005). On the other hand, mechanisms of heterogeneous catalysis are complex. Possible rate-determining steps include reactant transport to the catalyst, reactant adsorption, reactant surface diffusion, intrinsic reaction and secondary reactions, product surface diffusion, product desorption, product transport from the catalyst and catalyst deactivation or restructuring (Minh and Brown, 2006). In the literature, studies in the CO oxidation were reported over different catalysts.

Shalabi *et al.* (1995) suggested the models for rate of CO oxidation over Pt/CeO<sub>2</sub> catalyst. They used Langmuir-Hinshelwood rate expressions in order to fit the oxidation data and indicated that oxygen adsorbed on the interfacial sites of Pt/Ce and ceria lattice oxygen provided oxygen for an oxidation reaction as follows:



where “■” is an adsorption site and “●” a ceria lattice. The best of all the models fitted to the data in this work at excess oxygen concentrations was found as follows:

$$r_{CO} = \frac{kK_{O_2}^{1/2} K_{CO} K_{CO_2} P_{O_2}^{1/2} P_{CO} P_{CO_2}}{[1 + K_{O_2}^{1/2} P_{O_2}^{1/2} + K_{CO} P_{CO} + K_{CO_2} P_{CO_2}]^2} \quad (2.14)$$

Akın *et al.* (2001) suggested two alternative reaction paths for CO oxidation over Pt-SnO<sub>2</sub>/γ-Al<sub>2</sub>O<sub>3</sub> in the absence of CO<sub>2</sub> and H<sub>2</sub>O in the feed. On the basis of the kinetic analysis, they found the most plausible mechanism to be CO oxidation at the Pt/SnO<sub>2</sub> interface between adjacently chemisorbed CO and O<sub>2</sub>, with the reversible dissociative adsorption of O<sub>2</sub>, being the rate-determining step. The mechanism was given as follows:



where “■” refers to the Pt sites, and “\*” refers to the SnO<sub>2</sub> sites. The following rate expression is obtained using the concept of the most abundant reactive surface species and hence neglecting the surface concentration of oxygen in the adsorption term:

$$-r_{CO} = \frac{kP_{O_2}}{(1 + K_1 P_{CO})^2} \quad (2.18)$$

Oran and Uner (2004) investigated the reaction orders of CO and O<sub>2</sub> over the Pt/CeO<sub>2</sub> catalysts in the absence of CO<sub>2</sub> and H<sub>2</sub>O in the feed. The orders of CO and O<sub>2</sub> were found as -1 and 0, respectively that indicated a CO poisoned mechanism. They suggested that over the Pt/CeO<sub>2</sub> catalyst, reaction proceeds through the adsorbed CO and oxygen adatoms which are first dissociatively adsorbed on ceria surface and then reverse-spilled over the platinum surface where, the reverse spill over oxygen adatom to platinum surface is the rate-determining step and CO is the most abundant surface species. The surface reactions were depicted as follows:



where “■” refers to the Pt sites, and “●” refers to the ceria sites. As a result, the reaction rate takes the following form:

$$r_{\text{CO}_2} = \frac{k_2^f \theta_{\text{O}\bullet}}{1 + K_1 P_{\text{CO}}} \quad (2.23)$$

where “ $\theta_{\text{O}\bullet}$ ” is the surface coverage of oxygen over ceria. Reaction mechanisms for low-temperature CO oxidation in H<sub>2</sub> rich streams were also investigated as well as the low-temperature CO oxidation.

Pozdnyakova *et al.* (2006a) proposed a feasible mechanism for CO oxidation in PROX mixture is as follows. At the beginning, a significant amount of water accumulates on the ceria via spillover of adsorbed hydrogen atoms from the platinum. This water reacts in a low-temperature water gas shift reaction with linearly bonded CO at the Pt-ceria interface, forming CO<sub>2</sub> and H<sub>2</sub>. Hydrogen instead of desorption regenerates surface water by reacting with oxygen. At high temperature, the hydrogen-bonded structure decomposes

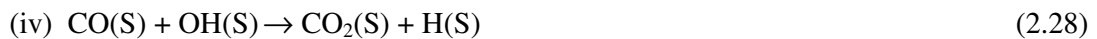
and water desorbs. As a result, CO can bind in bridged-like manner at the interface, giving rise to dissociation and/or formate formation. Thereafter, the empty interface site can be quickly refilled by a new CO molecule, continuing this side reaction. Although surface formates as intermediates in PROX cannot be completely excluded, they seem to represent a rather dead end for the reaction.

Kahlich *et al.* (1997) studied the kinetics of selective CO oxidation in H<sub>2</sub> rich gas over Pt/Al<sub>2</sub>O<sub>3</sub> and found the reaction orders of -0.4 for  $P_{CO}$  and +0.8 for  $P_{O_2}$  at an apparent activation energy of 71 kJ.mol<sup>-1</sup>. According to these reaction orders, it was suggested the selective CO oxidation reaction occurs in the low-rate branch that means the Pt surface is thought to be completely covered by CO, with dissociative O<sub>2</sub> adsorption being the rate limiting step. They obtained the rate expression by applying the power law:

$$-r_{CO} = k(P_{CO})^{0.4} \left( \frac{2P_{O_2}}{P_{CO}} \right)^{0.82} \quad (2.24)$$

Kahlich *et al.* (1997) also studied the Au/ $\alpha$ -Fe<sub>2</sub>O<sub>3</sub> catalyst and found positive reaction orders for both CO and O<sub>2</sub> at the reaction temperature of 80°C.

Kolb *et al.* (2007) studied the simulations of the reaction system for PROX. It revealed that CO oxidation occurs by the reaction between adsorbed CO and OH species and not by the reaction between adsorbed CO and O species. They formulated a simplified reaction mechanism as follows.



where “(S)” refers to the surface.

Plausible elementary reactions constituting the CO oxidation mechanism proposed in literature are given in Table 2.1, where “■” represents the Pt sites, and “●” represents the ceria sites.

Table 2.1. Plausible elementary reaction steps for the CO oxidation mechanism

Elementary Reaction Steps	References
$\text{CO} + \blacksquare \rightleftharpoons \text{CO}\blacksquare$	Oran and Uner, 2004
$\text{O}_2 + \blacksquare \rightarrow \text{O}_2\blacksquare$	Nibbelke <i>et al.</i> , 1998
$\text{CO} + \text{O}\blacksquare \rightleftharpoons \text{OCO}\blacksquare$	Nibbelke <i>et al.</i> , 1998
$\text{OCO}\blacksquare \rightarrow \text{CO}_2 + \blacksquare$	Nibbelke <i>et al.</i> , 1998
$\text{CO}\blacksquare + \text{O}\blacksquare \rightarrow \text{CO}_2 + 2\blacksquare$	Oran and Uner, 2004
$\text{O}_2 + \bullet \rightarrow \text{O}_2\bullet$	Nibbelke <i>et al.</i> , 1998
$\text{O}_2 + 2\bullet \rightarrow 2\text{O}\bullet$	Oran and Uner, 2004
$\text{O}_2\bullet + \bullet \rightarrow 2\text{O}\bullet$	Nibbelke <i>et al.</i> , 1998
$\text{CO}\blacksquare + \text{O}\bullet \rightarrow \text{CO}_2 + \blacksquare + \bullet$	Nibbelke <i>et al.</i> , 1998
$\text{H}_2 + 2\blacksquare \rightleftharpoons 2\text{H}\blacksquare$	Tibiletti <i>et al.</i> , 2004
$2\text{H}\blacksquare + \text{O}\blacksquare \rightarrow \text{H}_2\text{O} + 2\blacksquare$	Tibiletti <i>et al.</i> , 2004
$2\text{H}\bullet + \text{O}\bullet \rightarrow \text{H}_2\text{O}\bullet + 2\bullet$	Rajasree <i>et al.</i> , 2004
$\text{H}_2\text{O} + \bullet \rightleftharpoons \text{H}_2\text{O}\bullet$	Rajasree <i>et al.</i> , 2004
$\text{H}_2\text{O}\bullet + \text{O}\bullet \rightleftharpoons 2\text{OH}\bullet$	Rajasree <i>et al.</i> , 2004
$\text{CO}\blacksquare + \text{OH}\bullet \rightarrow \text{CO}_2 + \text{H}\bullet + \blacksquare$	Rajasree <i>et al.</i> , 2004

In the literature, reaction orders determined with respect to  $P_{\text{CO}}$  and  $P_{\text{O}_2}$  for CO oxidation on supported and single-crystalline platinum are also available and they are listed in Table 2.2. On the other hand, kinetic studies of CO oxidation over activated carbon supported catalysts are not reported.

Table 2.2. Reaction orders with respect to  $P_{CO}$  ( $\alpha_{CO}$ ) and  $P_{O_2}$  ( $\alpha_{O_2}$ ) for CO oxidation on supported and single-crystalline platinum at atmospheric pressure  
(Kahlich *et al.*, 1997; Oran and Uner, 2004)

System	Reaction Conditions	T-range (°C)	$\alpha_{CO}$	$\alpha_{O_2}$
Pt (111)	10 Torr CO:O <sub>2</sub>	50-157	0	+1
Pt (100)	8 Torr CO, $\lambda=1$	$\leq 170$	-0.6 to 0	+1
Pt/ $\gamma$ -Al <sub>2</sub> O <sub>3</sub>	0.38-7.6 Torr CO; $\lambda=2$ ; 75% H <sub>2</sub>	150-250	-0.4	+0.8
Pt/ $\gamma$ -Al <sub>2</sub> O <sub>3</sub>	7.6 Torr CO, $\lambda=1$	<200	-1.5	+1
Pt/ $\gamma$ -Al <sub>2</sub> O <sub>3</sub>	23 Torr CO, $\lambda=1$	100–220	-0.1	+0.7
Pt/SiO <sub>2</sub>	10 Torr CO, $\lambda=1$	<150	-0.2	+0.9
Pt/CeO <sub>2</sub> / $\gamma$ -Al <sub>2</sub> O <sub>3</sub>		$\leq 200$	-0.6 to 1	0 to 0.9
Pt-Rh/CeO <sub>2</sub> / $\gamma$ -Al <sub>2</sub> O <sub>3</sub>	0.9-62 Torr CO and O <sub>2</sub> ; 0-75 Torr H <sub>2</sub> O and CO <sub>2</sub>	163-230	-0.3	+0.5

It is apparent from the data presented in Table 2.2 that the oxygen orders over Pt surfaces do not depend on the presence of Al<sub>2</sub>O<sub>3</sub>, but the reaction orders with respect to oxygen show a tendency to decrease in the presence of CeO<sub>2</sub>. On the other hand, reaction orders with respect to CO change in the range of -1.5 to 0.0 over unsupported and Al<sub>2</sub>O<sub>3</sub> supported catalysts. It can also be seen from Table 2.2 that reaction orders for O<sub>2</sub> change in the range of 0 to 1. Kahlich *et al.* (1997) reported that according to the review by Engel and Ertl these reaction orders are suitable for the low rate branch in which the surface is predominantly covered with adsorbed CO.

### 3. EXPERIMENTAL WORK

#### 3.1. Materials

##### 3.1.1. Chemicals

The chemicals used for catalyst preparation are listed in Table 3.1.

Table 3.1. Chemicals used in catalyst preparation

Chemicals	Formula	Grade	Source	Molecular Weight (g/mole)
Hexachloroplatinic acid	$\text{H}_2\text{PtCl}_6 \cdot 6\text{H}_2\text{O}$	Extra pure	Carlo Erba	517.92
Cerium(III) nitrate hexahydrate	$\text{Ce}(\text{NO}_3)_3 \cdot 6\text{H}_2\text{O}$	Extra Pure	Merck	434.23
Activated Carbon	C	ROX 0.8	NORIT	12
Hydrochloric Acid	HCl	Research	Merck	36.46

##### 3.1.2. Gases

All of the gases used in this study are listed with their applications and specifications in the Tables 3.2 and were obtained from BOS and HABAŞ Companies, Istanbul, Turkey.

Table 3.2. Applications and specifications of the gases used

Gas/Standard	Application	Specification
Nitrogen	Catalyst preparation	99.99% BOS
Dry air	Catalyst preparation	99.99% BOS
Carbon monoxide	Reactant, GC calibration	99.0% HABAŞ
70.3 vol. % oxygen in helium	Reactant	BOS
Carbon dioxide	Reactant	99.99% BOS
Hydrogen	Reactant, reducing agent	99.99% BOS
Helium	Reactant (Inert)	99.99% BOS
Helium	GC Carrier	99.99% BOS

### 3.2. Experimental Setup

The experimental systems used for catalyst preparation and reaction tests as well as kinetic studies can be described in three groups:

- Catalyst Preparation System: this system is used for catalyst preparation by sequential impregnation method.
- Microreactor flow system: this system consists of automated reactant flow system and a temperature controlled reactor.
- Product analysis system: this system is connected to the microreactor flow system and consists of a gas sampling section, a gas chromatograph and a data processor. The gas chromatograph is used for determining concentrations of feed gases and reaction products on line.

### 3.2.1. Catalyst Preparation System

Activated carbon supported 1wt.%Pt-1wt.%CeO<sub>x</sub> catalyst was prepared by impregnation method using the system presented in Figure 3.1 in this study.

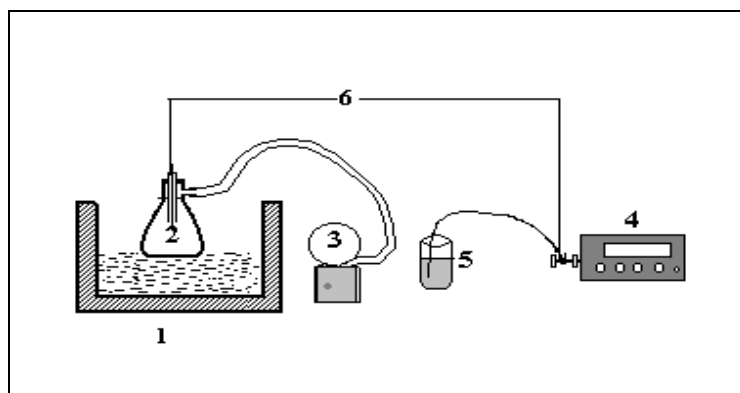


Figure 3.1. The impregnation system: 1.Ultrasonic mixer 2.Vacuum flask  
3.Vacuum pump 4.Peristaltic pump 5.Beaker 6.Silicone tubing

### 3.2.2. Microreactor Flow System

1/4" and 1/8" OD stainless steel or brass tubing and fittings and research grades of pure CO, CO<sub>2</sub>, H<sub>2</sub>, He gases and O<sub>2</sub>/He mixture were used in the system. Flow rates of these gases were controlled using four Brooks 5850E mass flow controllers and one Aalborg GFC mass flow controller (for CO<sub>2</sub>). All gases, after being mixed, were sent into the reaction section which consists of a 4 mm. ID stainless steel fixed-bed down-flow microreactor located in a 2.4 cm ID x 40 cm furnace controlled to  $\pm 0.5$  K by a Shimaden FP-21 programmable temperature controller. The total length of the reactor was 53 cm, which is longer than the furnace to facilitate manipulation during catalyst charging or recharging. The catalyst bed was placed in the middle of the reactor tube in the constant temperature region of the furnace. A 1/16" K- type stainless steel sheathed thermocouple is placed adjacent to the middle point of the catalyst bed just outside the microreactor. The spaces between inlet of the reactor-furnace and the outlet of the reactor-furnace were closed by ceramic wool to prevent heat loss and maintain stable temperature profile. In the reactant and product sampling section, the reactant mixture entering or the product leaving

the reactor were passed through two on-off valves to either the gas chromatograph sampling unit which has a calibrated 1 ml sample loop for analysis or to the soap bubblemeter for measuring the flow rate of the effluent at the ambient temperature. The microreactor flow and product analysis system is shown in Figure 3.2.

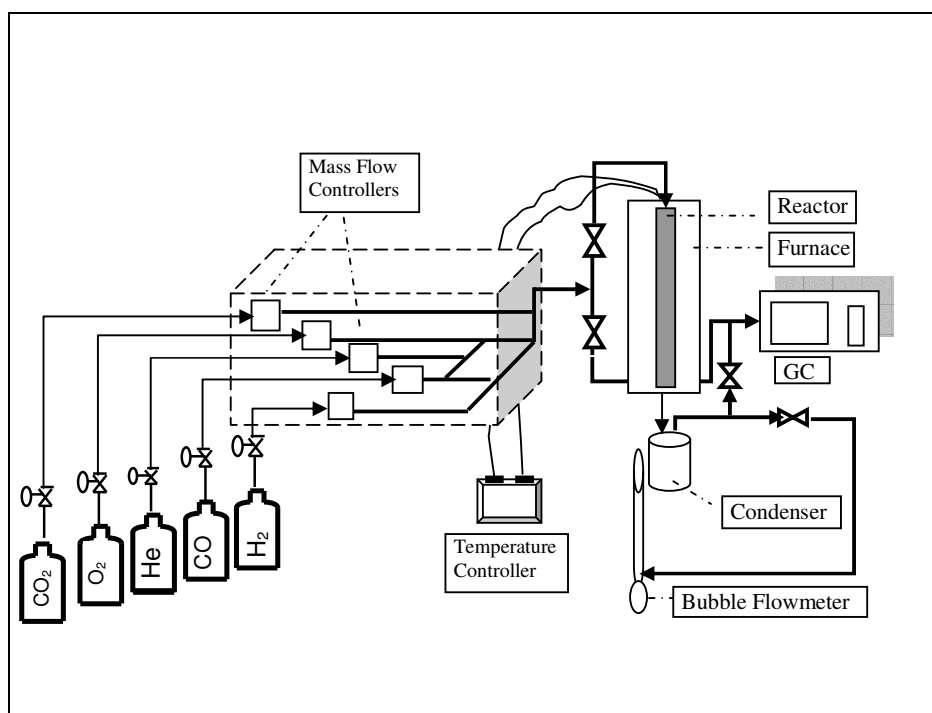


Figure 3.2. The microreactor flow and product analysis system

### 3.2.3. Product Analysis System

Reactant and product streams were analyzed using an ATI UNICAM 610 Series, temperature-controlled and programmable gas chromatograph equipped with a thermal conductivity detector (TCD), ATI UNICAM 4815 Computing Integrator and CTR I concentric column operating at 30°C under 35 cm<sup>3</sup>/min helium as carrier. Analysis conditions are given in Table 3.3.

Table 3.3. Reactant and product gas analysis conditions

Column Type	CTR I (Concentric Column)
Outer Column Packing	Activated Molecular Sieve
Inner Column Packing	Porous Polymer Mixture
Column Oven Temperature	303 K
Carrier Gas	Helium
Carrier Gas Flow Rate	35 ml/min
Detector Type	Thermal Conductivity
Detector Current	120 mA
Filament Temperature	513 K (Low sensitivity)
Detector Oven Temperature	413 K
Injector Oven Temperature	323 K

### 3.3. Catalyst Preparation

The activated carbon supported catalyst was prepared by sequential impregnation. It contained 1 wt.%Pt, 1 wt.%CeO<sub>x</sub>. A commercial activated carbon (AC) was used as a support after washing with HCl and further oxidation with air aiming at the enhancement of its textural and surface chemical characteristics.

#### 3.3.1. Pretreatment of the Activated Carbon Support

A commercial activated carbon, Norit ROX, was crushed and sieved into 45-60 mesh size (344-255 μm) and exposed to different thermal and chemical pretreatments indicated below prior to use.

Firstly, activated carbon material was treated with 2N HCl of 200 ml acid solution to remove some ash content and accompanying sulfur. This treatment was carried out in a Soxhlet apparatus. Approximately 15 g of the commercial activated carbon was placed in an extraction unit held by a cellulosic cup. Extraction process was continued under reflux for 12 h. After that, the slurry was rinsed with 250 ml distilled water and washed again

inside the Soxhlet apparatus for 6 h to remove HCl remaining on the support surface. Finally, the slurry was dried at 388 K overnight. This support is called AC1.

AC1 support was oxidized in a down-flow reactor according to a procedure which involves heating the AC1 from room temperature to 723 K at 10 K/min heating rate under 150 ml/min N<sub>2</sub> flow, keeping it at 723 K for 10 h under the flow of 150 ml/min N<sub>2</sub> + 50 ml/min dry air mixture and cooling the sample down to the room temperature under the flow of 150 ml/min N<sub>2</sub>. The second type of air-oxidized AC support thus obtained is called AC2.

### 3.3.2. Impregnation Method

The experimental setup shown in Figure 3.1 was used for preparation of 1%Pt-1%CeO<sub>x</sub> supported on air-oxidized activated carbon. The impregnation procedure comprises three steps. These are:

- Evacuating the support
- Contacting the support with the precursor solution
- Drying

For incipient wetness impregnation, 5 grams of activated carbon was placed in a vacuum flask and kept under vacuum both before and during the addition of precursor solutions. Thus, trapped air in pores of the support that could prevent penetration of the precursor solution was eliminated. The vacuum pump was used to remove the trapped air and to give a uniform distribution of the active component. Before impregnating the precursor solution, the support material was mixed with ultrasonic mixer for 25 min.

A Masterflex computerized-drive peristaltic pump was used to feed the precursor solution to the vacuum flask at a rate of 5 mL/min via silicone tubing. The slurry was mixed by an ultrasound mixer during the impregnation in order to maintain uniform distribution of the precursor solutions. After the precursor solution was added, the slurry was ultrasonically mixed for an additional 90 min. The thick slurry obtained was dried at 115°C overnight.

Bimetallic Pt-CeO<sub>x</sub>/AC catalyst with the 1 wt.% Pt and 1 wt.% CeO<sub>x</sub> loads was prepared by sequential impregnation (Ce+Pt). Firstly, aqueous cerium nitrate solution was impregnated and it was followed by impregnation of aqueous hexachloroplatinic acid solution. After the each impregnation step, the sample was dried overnight at 115°C and then stored in a desiccator.

Activated carbon supported Pt-CeO<sub>x</sub> catalysts were previously prepared by Özkara (2002) with sequential impregnation in which impregnation of cerium nitrate solution was followed by heat treatment under He flow at 673 K and then by impregnation of aqueous hexachloroplatinic acid solution in order to make characterization and performance tests for CO oxidation and also these catalysts were used by Şimşek for the investigation of effect of CO<sub>2</sub> and (CO<sub>2</sub>+H<sub>2</sub>O) on H<sub>2</sub>-rich CO oxidation. On the other hand, in this study, hexachloroplatinic acid solution was impregnated after the impregnation of cerium nitrate solution without heat treatment under He flow.

### 3.4. Kinetic Measurements

The temperature program used for the reductive pretreatment of the 1 wt.% Pt-1 wt.% CeO<sub>x</sub>/AC2 is given in Table 3.4.

Table 3.4. Reduction program for Pt-CeO<sub>x</sub>/AC2 catalyst

Segments	Starting and End Temperatures	Segment Gas
First	Heating from 293 K to 393 K with a heating rate 10 K/min	He with flow rate of 50 ml/min
Second	Keeping constant at 393 K for 20 min	He with flow rate of 50 ml/min
Third	Heating from 393 K to 673 K with a heating rate 10 K/min	He with flow rate of 50 ml/min
Fourth (Calcination)	Keeping constant at 673 K for 2 hours	He with flow rate of 50 ml/min
Fifth (Reduction)	Keeping constant at 673 K for 2 hours	H <sub>2</sub> with flow rate of 50 ml/min
Sixth	Sweeping at 673 K for 1 hour	He with flow rate of 50 ml/min

The CO oxidation reaction on Pt-CeO<sub>x</sub>/AC2 catalyst was investigated over a relatively wide range of CO concentrations (1-5 per cent) at 383 K reaction temperature. Different sets of CO and O<sub>2</sub> concentrations each at different space times and catalyst loadings (100,150, 200 and 250 mg) were used in kinetic measurements. In the absence of hydrogen, molar reactant concentrations in the feed were varied between 1-5 per cent CO and 1-2.5 per cent O<sub>2</sub>. In mixed-feed experiments, the CO<sub>2</sub> concentration in the feed was changed in the range of 2-5 per cent by keeping the feed composition of CO and O<sub>2</sub> at 5 per cent and 2.5 per cent, respectively. In preferential CO oxidation experiments, the H<sub>2</sub> concentrations used were between 5-60 per cent in order to investigate the effect of the presence of H<sub>2</sub> in the feed on CO oxidation rates.

The reaction conditions for the catalyst in the absence of CO<sub>2</sub> and H<sub>2</sub> and in the presence of either CO<sub>2</sub> or H<sub>2</sub> were given in Tables 3.5 and 3.6, respectively.

Table 3.5. The reaction conditions studied over air oxidized activated carbon supported Pt-CeO<sub>x</sub> catalyst in the absence of CO<sub>2</sub> and H<sub>2</sub>

Exp. No	T <sub>rxn</sub> (°C)	Total Flow (ml/min)	Weight of Catalyst (mg)	Feed Composition (%) with He as Balance			
				CO	O <sub>2</sub>	CO <sub>2</sub>	H <sub>2</sub>
1	110	100	150	1	1	-	-
2	110	150	150	1	1	-	-
3	110	150	100	1	1	-	-
4	110	150	150	2	1	-	-
5	110	150	100	2	1	-	-
6	110	150	250	2	1	-	-
7	110	150	200	2	1	-	-
8	110	100	250	2	1	-	-
9	110	100	200	2	1	-	-
10	110	150	200	3	1	-	-
11	110	100	250	3	1	-	-
12	110	100	200	3	1	-	-
13	110	150	250	3	1.5	-	-
14	110	100	250	3	1.5	-	-
15	110	100	200	3	1.5	-	-
16	110	100	200	4	2	-	-
17	110	100	250	5	2	-	-
18	110	100	200	5	2	-	-
19	110	150	250	5	2.5	-	-
20	110	150	200	5	2.5	-	-

Table 3.6. The reaction conditions studied over air oxidized activated carbon supported Pt-CeO<sub>x</sub> catalyst in the presence of CO<sub>2</sub> or H<sub>2</sub>

Exp. No	T <sub>rxn</sub> (°C)	Total Flow (ml/min)	Weight of Catalyst (mg)	Feed Composition (%) with He as Balance			
				CO	O <sub>2</sub>	CO <sub>2</sub>	H <sub>2</sub>
21	110	150	250	5	2.5	2.0	-
22	110	150	250	5	2.5	2.5	-
23	110	150	250	5	2.5	3.0	-
24	110	150	250	5	2.5	3.5	-
25	110	150	200	5	2.5	4.0	-
26	110	150	250	5	2.5	-	5
27	110	150	250	5	2.5	-	10
28	110	150	250	5	2.5	-	15
29	110	150	250	5	2.5	-	20
30	110	150	250	5	2.5	-	40
31	110	150	250	5	2.5	-	60

## 4. RESULTS AND DISCUSSION

### 4.1. Introduction

The selective oxidation of CO over various HNO<sub>3</sub>- and air-oxidized activated carbon (AC) supported 1wt.%Pt-1wt.%CeO<sub>x</sub> catalysts was studied by Özkara (2002) in order to determine one or more catalysts that had sufficient low-temperature PROX activity. The effects of the presence of CO<sub>2</sub> and water in the feed on the reaction were later studied on the same catalysts by Şimşek (2005). 1wt.%Pt-1wt.%CeO<sub>x</sub> supported on air-oxidized AC (AC2) was selected as an efficient catalyst that may be a potential candidate for commercial use.

In the present work, the kinetics of low-temperature CO oxidation on air-oxidized activated carbon supported 1wt.%Pt-1wt.%CeO<sub>x</sub> was studied over a relatively wide range of CO concentrations (1-5 per cent) at low stoichiometric O<sub>2</sub> excess ( $P_{O_2} / P_{CO} = 0.3-1.0$ ) in the initial rate region and at a constant temperature of 383 K. The effect of both CO<sub>2</sub> and H<sub>2</sub> on CO oxidation were also investigated by varying their concentrations while keeping the CO and O<sub>2</sub> concentrations constant in the feed. This study focuses on the determination of a power-function rate expression for low-temperature CO oxidation; Langmuir-Hinshelwood rate expressions that are plausible on the basis of experimental data are also put forward.

The conversions of CO and O<sub>2</sub> were defined as follows:

$$\text{CO conversion (\%)} = \frac{[CO]_{in} - [CO]_{out}}{[CO]_{in}} \times 100 \quad (4.1)$$

$$\text{O}_2 \text{ conversion (\%)} = \frac{[O_2]_{in} - [O_2]_{out}}{[O_2]_{in}} \times 100 \quad (4.2)$$

The catalyst mass-based reaction rates in the kinetic measurements,  $(-r_{CO})$ , can be calculated from the conversion versus residence time ( $W_{cat}/F_{CO_{in}}$ ) data as follows:

$$-r_{CO} = \frac{x_{CO}F_{CO_{in}}}{W_{cat}} \quad (4.3)$$

where  $x_{CO}$  is CO conversion,  $F_{CO_{in}}$  is CO flow rate in the feed in  $\text{ml}\cdot\text{min}^{-1}$  converted to  $\mu\text{mol}\cdot\text{s}^{-1}$ ,  $W_{cat}$  is catalyst weight in g and  $(-r_{CO})$  is the reaction rate in  $\mu\text{mol}\cdot\text{g}^{-1}\cdot\text{s}^{-1}$ . In order to justify this assumption, the CO conversion has to be kept well below 10 per cent in these measurements which are performed under differential flow conditions. It is reported that the differential reactor approximation could be used at conversions lower than 10 per cent to calculate reaction rates (Nibbelke *et al.*, 1997; Kim and Lim, 2002).

CO consumption rates were obtained from intrinsic kinetic data in the initial rate region by using the differential method of data analysis. The use of differential method of data analysis to determine reaction orders and specific reaction rates is clearly one of the easiest methods. By varying the ratio of  $W/F_{CO}$ , a wide range of conversions can be obtained. In the method of initial rates, a series of experiments were carried out at different initial reactant concentrations. The initial rate can be calculated by differentiating the data and extrapolating to zero time. In this study, kinetic measurements were carried out at 383 K in order to obtain low CO conversion levels that are required for the application of the initial rates method.

## 4.2. Kinetic Study of CO Oxidation

### 4.2.1. Low-Temperature CO Oxidation

The dependence of CO oxidation rate on CO and O<sub>2</sub> partial pressures over air-oxidized activated carbon supported 1%Pt-1%CeO<sub>x</sub> catalyst was first studied in the absence of CO<sub>2</sub> and H<sub>2</sub> in the feed stream. The measurements were taken at 383 K for the

determination of reaction orders with respect to CO and O<sub>2</sub> by varying the CO and O<sub>2</sub> concentrations in the feed and the residence time.

CO conversions obtained at 90 minutes time-on-stream (TOS) were used for the kinetic calculations. Representative fractional CO conversions obtained at 30, 60, 90 and 120 min are shown in Figure 4.1 for O<sub>2</sub>/CO inlet ratios of 1.0 and 0.5 at  $W/F_{CO}$  values of 0.220 and 0.122 g.s.μmol<sup>-1</sup>, respectively. A total of 23 duplicated runs were conducted; conversion data obtained at constant composition by varying the  $W/F_{CO}$  ratio were fitted with straight lines passing through the origin (see Appendix A). This was done both to verify operation in the initial rates region and to eliminate definite outliers in data. The CO conversions obtained in 20 duplicate experiments over 1%Pt-1%CeO<sub>x</sub>/AC2 catalyst at 383 K in the presence of CO, O<sub>2</sub> and balance He in the feed are given in Table 4.1.

The O<sub>2</sub>/CO ratio is a key factor for the state of the catalyst surface and, therefore, also for the reaction mechanism and kinetics. Excess CO in the feed causes the activity to decrease because of CO poisoning of active sites. This is supported by the results of activity experiments given in Table 4.1 for O<sub>2</sub>/CO inlet ratios <0.50. In this study, O<sub>2</sub>/CO ratio was varied between 0.33-1 which means that ratios both lower and higher than the stoichiometric were selected for studying the CO oxidation reaction.

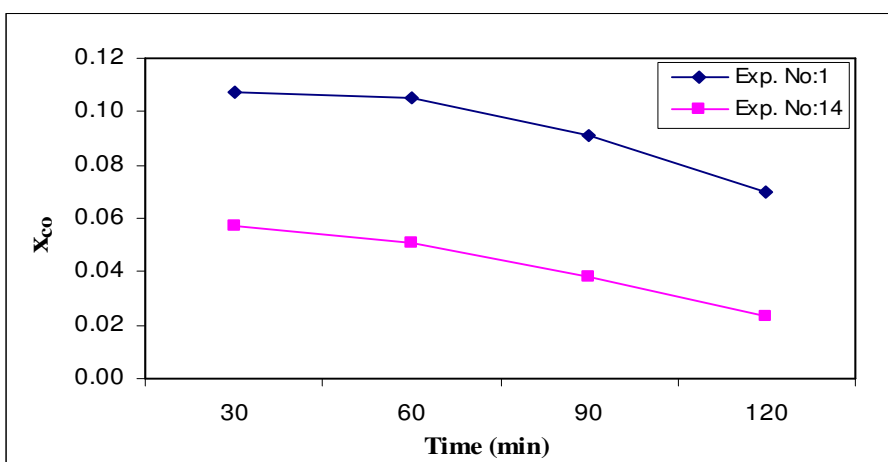


Figure 4.1. Fractional CO conversion versus time for experiments 1 and 14 conducted under conditions defined in Table 4.1.

Table 4.1. CO conversions over 1%Pt-1%CeO<sub>x</sub>/AC2  
with He as balance in the absence of CO<sub>2</sub> and H<sub>2</sub>, T = 383 K

Exp. No	CO %	O <sub>2</sub> %	O <sub>2</sub> /CO	$F_T$ (ml/min)	$W_{cat}$ (mg)	Fractional conversion at 90 min TOS
						$x_{CO}$
1	1	1	1	100	150	0.091
2	1	1	1	150	150	0.048
3	1	1	1	150	100	0.042
4	2	1	0.5	150	150	0.043
5	2	1	0.5	150	100	0.028
6	2	1	0.5	150	250	0.056
7	2	1	0.5	150	200	0.018
8	2	1	0.5	100	250	0.053
9	2	1	0.5	100	200	0.045
10	3	1	0.33	150	200	0.008
11	3	1	0.33	100	250	0.039
12	3	1	0.33	100	200	0.034
13	3	1.5	0.5	150	250	0.037
14	3	1.5	0.5	100	250	0.038
15	3	1.5	0.5	100	200	0.021
16	4	2	0.5	100	200	0.040
17	5	2	0.4	100	250	0.034
18	5	2	0.4	100	200	0.035
19	5	2.5	0.5	150	250	0.052
20	5	2.5	0.5	150	200	0.016

4.2.1.1. Rate Calculations. The rate expression most commonly applied to the CO oxidation reaction is a simple power-law functionality in the initial rate region:

$$(-r_{co})_o = k (P_{co})^\alpha (P_{o_2})^\beta \quad (4.4)$$

Evaluation of the rate parameters requires firstly the determination of the reaction rates on the left-hand side of Equation 4.4. The reaction rates were calculated using Equation 4.3 with the corresponding conversion versus  $W/F_{CO}$  data given in Table 4.1. The flow rates of the CO and O<sub>2</sub> were converted to concentrations in mole per cent which were equivalent to reactant partial pressures as the operation pressure was atmospheric. The resulting rate versus partial pressure data given in Table 4.2 were processed using nonlinear regression analysis. The Levenberg-Marquardt algorithm provided in the computer software POLYMATH 5.1 was used in order to estimate the parameters,  $k$ ,  $\alpha$  and  $\beta$  of Equation 4.4

The Levenberg-Marquardt algorithm is an iterative technique that locates the minimum of a function that is expressed as the sum of squares of nonlinear functions. The sum of the squared differences of the measured reaction rates,  $(-r)_m$ , and the calculated reaction rates,  $(-r)_c$ , for N experiments (=20) and p parameter values (=3) is defined as variance of experimental error given by the following equation:

$$\sigma^2 = \sum_{i=1}^n \frac{[(-r)_{im} - (-r)_{ic}]^2}{(N - p)} \quad \rightarrow \quad \text{minimum} \quad (4.5)$$

Table 4.2. Partial pressures of CO and O<sub>2</sub> and calculated initial rates over 1%Pt-1%CeO<sub>x</sub>/AC2 in the absence of CO<sub>2</sub> and H<sub>2</sub>, T = 383 K

Experiment No	Partial Pressures (atm)		$W_{cat}/F_{COin}$ (g.s.μmol <sup>-1</sup> )	$(-r_{CO})_o$ (μmol.g <sup>-1</sup> .s <sup>-1</sup> )
	CO	O <sub>2</sub>		
1	0.01	0.01	0.220	0.4135
2	0.01	0.01	0.147	0.3271
3	0.01	0.01	0.098	0.4294
4	0.02	0.01	0.073	0.5861
5	0.02	0.01	0.049	0.5725
6	0.02	0.01	0.122	0.4580
7	0.02	0.01	0.098	0.1840
8	0.02	0.01	0.183	0.2890
9	0.02	0.01	0.147	0.3067
10	0.03	0.01	0.065	0.1227
11	0.03	0.01	0.122	0.3190
12	0.03	0.01	0.098	0.3476
13	0.03	0.015	0.082	0.4539
14	0.03	0.015	0.122	0.3108
15	0.03	0.015	0.098	0.2147
16	0.04	0.02	0.073	0.5452
17	0.05	0.02	0.073	0.4635
18	0.05	0.02	0.059	0.5964
19	0.05	0.025	0.049	1.0632
20	0.05	0.025	0.039	0.4089

The reaction orders with respect to CO ( $\alpha$ ) and O<sub>2</sub> ( $\beta$ ) are found as  $-0.29$  and  $1.07$ , respectively, using POLYMATH computer software. The reaction rate constant,  $k$ , is determined as  $14.7 \mu\text{mol.g}^{-1}.\text{s}^{-1}.\text{atm}^{-0.78}$ . Consequently, the power-function rate expression for low-temperature CO oxidation over air-oxidized activated carbon supported 1%Pt-1%CeO<sub>x</sub> catalyst at 383 K in the initial rate region can be given as:

$$(-r_{co})_o = 14.7(P_{co})^{-0.29}(P_{o_2})^{1.07} \quad (4.6)$$

The variance of experimental error is found to be  $0.03 (\mu\text{mol.g}^{-1}.\text{s}^{-1})^2$  for this rate expression.

Three reaction regimes have been described for CO oxidation: (i) a regime controlled by the intrinsic reaction kinetics, characterized by a negative carbon monoxide reaction order and a positive reaction order close to one for oxygen; (ii) a second regime described as a regime in which the conversion is influenced by both mass transfer and reaction kinetics, and where the apparent reaction order in CO can be lower than  $-1$ , while that for  $\text{O}_2$  can be higher than  $+1$  (Venderbosch *et al.*, 1998); (iii) a third regime where mass transfer resistances are dominant and the apparent reaction order in CO has a value of  $+1$  and that in  $\text{O}_2$  is zero. The mass transfer effects were totally eliminated in the present experiments by selecting suitable flowrate and particle size values (Özkara, 2003). The reaction rate measurements also confirm the first regime where reaction kinetics is rate controlling.

Power-law rate expressions can be obtained from Langmuir-Hinshelwood mechanisms under particular conditions. According to the Langmuir-Hinshelwood mechanism, carbon monoxide and oxygen are both adsorbed at the surface of the catalyst, where the reaction towards carbon dioxide takes place (Venderbosch *et al.*, 1998). The orders in CO and  $\text{O}_2$  obtained in this study are in good agreement with the results obtained by other authors. Venderbosch *et al.* (1998) studied on CO oxidation in the pure feed ( $\text{CO}+\text{O}_2+\text{N}_2$ ) over  $\text{Pt}/\gamma\text{-Al}_2\text{O}_3$  and found the orders of CO and  $\text{O}_2$  as  $-1$  and  $+1$ , respectively. The reaction orders of CO and  $\text{O}_2$  were found approximately as  $-1.0$  and  $0.0$  over the  $\text{Pt}/\text{CeO}_2$  and  $\text{Pt}/\text{CeO}_2/\gamma\text{-Al}_2\text{O}_3$  catalysts, but as  $-2.0$  and  $+1.0$  over the  $\text{Pt}/\gamma\text{-Al}_2\text{O}_3$  catalyst, respectively by Oran and Uner (2004). They proposed that in the presence of  $\text{CeO}_2$ , the reaction orders with respect to oxygen show a tendency to decrease. The observation of zero-order oxygen pressure dependence is described as the participation of oxygen from the ceria support in CO oxidation (Wootsch *et al.*, 2004). Kahlich *et al.* (1997) reported that Cant *et al.* (1978) studied on the kinetics of CO oxidation over  $\text{Pt}/\text{SiO}_2$  at  $150^\circ\text{C}$  and the reaction orders with respect to CO and  $\text{O}_2$  were found as  $-0.2$  and  $0.9$ ,

respectively. The positive reaction order close to unity with respect to oxygen obtained in this study implies that relatively weak adsorption of oxygen is involved.

The combination of a negative value for CO and a positive value for O<sub>2</sub> points to a Langmuir-Hinshelwood mechanism, with the reaction limited by (dissociative) O<sub>2</sub> adsorption due to the presence of a dense CO adlayer (low rate branch) as it had been proposed or demonstrated for CO oxidation on many platinum metal surfaces or supported catalysts (Kahlich *et al.*, 1997).

In this study, Langmuir-Hinshelwood rate expressions were also used to fit the CO oxidation data obtained. No single rate expression can effectively describe the CO oxidation data over the entire range of CO concentrations. Experimental CO rate data were analyzed using nonlinear regression analysis with Levenberg-Marquardt algorithm provided in the computer software POLYMATH 5.1 for estimating parameters in the various kinetic models.

A model with smaller variance (Equation 4.5) is likely to represent the data more accurately than a model with larger values of this indicator. Models giving either poor correlation coefficients or negative parameter values were rejected during the estimation of the kinetic parameters. The proposed Langmuir-Hinshelwood type rate expressions are given in Table 4.3 using the initial guess of one for  $k$ ,  $K_{CO}$  and  $K_{O_2}$ .

The equation that best fits the experimental data can be determined by comparing the variance of the experimental error ( $\sigma^2$ ) for each model and selecting the equation with a smaller one (Fogler, 1999). The discrimination of kinetic models as illustrated in Table 4.3 indicates the Langmuir-Hinshelwood mechanism, as depicted in model no 1, to give the best result among the model equations fitted to the data in this work.

Table 4.3. Langmuir-Hinshelwood rate expressions tested for low-temperature CO oxidation in the absence of CO<sub>2</sub> and H<sub>2</sub> at 383 K

Model No	Proposed Rate Equations	Rate Parameters	$\sigma^2$ ( $\mu\text{mol.g}^{-1}.\text{s}^{-1}$ ) <sup>2</sup>
1	$(-r_{co})_o = \frac{kP_{o_2}}{(1 + K_{co}P_{co}^{1/2})}$	$k = 64 \mu\text{mol.g}^{-1}.\text{s}^{-1}.\text{atm}^{-1}$ $K_{co} = 6.4 \text{ atm}^{-1/2}$	0.028
2	$(-r_{co})_o = \frac{kP_{o_2}}{(1 + K_{co}P_{co})^2}$	$k = 40.7 \mu\text{mol.g}^{-1}.\text{s}^{-1}.\text{atm}^{-1}$ $K_{co} = 4.8 \text{ atm}^{-1}$	0.029
3	$(-r_{co})_o = \frac{kK_{co}P_{co}P_{o_2}}{(1 + K_{co}P_{co})^2}$	$k = 102 \mu\text{mol.g}^{-1}.\text{s}^{-1}.\text{atm}^{-1}$ $K_{co} = 36.5 \text{ atm}^{-1}$	0.041
4	$(-r_{co})_o = \frac{kK_{co}K_{o_2}P_{co}P_{o_2}}{(1 + K_{co}P_{co} + K_{o_2}P_{o_2})}$	$k = 5.2 \mu\text{mol.g}^{-1}.\text{s}^{-1}$ $K_{co} = 102 \text{ atm}^{-1}$ $K_{o_2} = 6.3 \text{ atm}^{-1}$	0.047

The kinetic measurements show that the CO reaction rate varied inversely with carbon monoxide partial pressure. Thus the partial pressure of CO appears in the denominator of these proposed Langmuir-Hinshelwood rate expressions. This proves that carbon monoxide was adsorbed on the surface. Relatively weak adsorption of oxygen is indicated by the reaction order of unity in this reaction. The results obtained in formulating a power-function rate expression are also in agreement with the Langmuir-Hinshelwood rate expressions.

Akin *et al.* (2001) indicated model no 2 for CO oxidation over Pt-SnO<sub>2</sub>/ $\gamma$ -Al<sub>2</sub>O<sub>3</sub> and proposed that CO oxidation on Pt sites or at the Pt-SnO<sub>2</sub> interface between adjacently chemisorbed CO and O<sub>2</sub>, with the dissociative adsorption of O<sub>2</sub> as the rate limiting step is the most plausible mechanism.

#### 4.2.2. Effect of CO<sub>2</sub> on Low-Temperature CO Oxidation

The dependence of CO oxidation rate over 1%Pt-1%CeO<sub>x</sub>/AC2 on CO<sub>2</sub> concentration was studied using feed containing 5 per cent CO, 2.5 per cent O<sub>2</sub> and different CO<sub>2</sub> percentages with balance He. The total flow rate used was 150 ml.min<sup>-1</sup> with a catalyst loading of 250 mg. The CO<sub>2</sub> concentration was varied from 2 per cent to 4 per cent. The CO and O<sub>2</sub> conversions obtained in five duplicated experiments are presented in Table 4.4.

Table 4.4. CO and O<sub>2</sub> conversions over 1%Pt-1%CeO<sub>x</sub>/AC2 in the presence of CO<sub>2</sub> with He as balance, T = 383 K

Exp. No	CO %	F <sub>CO</sub> (ml/min)	O <sub>2</sub> %	F <sub>O<sub>2</sub></sub> (ml/min)	CO <sub>2</sub> %	F <sub>CO<sub>2</sub></sub> (ml/min)	fractional conversions at 90 min TOS	
							x <sub>CO</sub>	x <sub>O<sub>2</sub></sub>
21	5	7.5	2.5	3.75	2.0	3.00	0.039	0.048
22	5	7.5	2.5	3.75	2.5	3.75	0.034	0.044
23	5	7.5	2.5	3.75	3.0	4.50	0.031	0.042
24	5	7.5	2.5	3.75	3.5	5.25	0.019	0.035
25	5	7.5	2.5	3.75	4.0	6.00	0.011	0.030

The results show that the CO conversion decreases from 5.2 per cent to 3.9 per cent with the addition of 2 per cent CO<sub>2</sub> to the 5 per cent CO, 2.5 per cent O<sub>2</sub> and balance He feed stream (Table 4.1, Experiment 19). Between CO<sub>2</sub> contents of 2 to 3 per cent, the change in CO conversion is gradual while it becomes more rapid after a CO<sub>2</sub> content of 3.5 per cent. O<sub>2</sub> conversion also drops with increasing CO<sub>2</sub> content.

4.2.2.1. Rate Calculations. The conversions obtained predict that the incorporation of partial pressure of CO<sub>2</sub> into the CO oxidation rate expression is necessary and will have an inhibitory effect. Thus, the power-function rate expression for CO oxidation becomes:

$$(-r_{CO})_o = k'(P_{CO})^\alpha (P_{O_2})^\beta (P_{CO_2})^\delta \quad (4.7)$$

Partial pressures of CO, O<sub>2</sub> and CO<sub>2</sub> in the feed and calculated initial reaction rate data used for evaluation of CO<sub>2</sub> reaction order are presented in Table 4.5. Low-temperature CO oxidation rates in the presence of CO<sub>2</sub> are also plotted versus partial pressure in Figure 4.2.

Table 4.5. Effect of CO<sub>2</sub> partial pressure on CO oxidation rates over  
1%Pt-1%CeO<sub>x</sub>/AC2 at T = 383 K

Exp. No	Partial Pressures (atm)			$W_{cat} / F_{CO_{in}}$ (g.s.μmol <sup>-1</sup> )	$(-r_{CO})_o$ (μmol.g <sup>-1</sup> .s <sup>-1</sup> )
	CO	O <sub>2</sub>	CO <sub>2</sub>		
21	0.05	0.025	0.020	0.049	0.7974
22	0.05	0.025	0.025	0.049	0.6952
23	0.05	0.025	0.030	0.049	0.6338
24	0.05	0.025	0.035	0.049	0.3885
25	0.05	0.025	0.040	0.049	0.2249

It can be seen in Figure 4.2 that the CO oxidation rate over 1%Pt-1%CeO<sub>x</sub>/AC2 decreases with increasing CO<sub>2</sub> partial pressure at 383 K, indicating that co-adsorbed CO<sub>2</sub> predominantly blocks sites active for CO oxidation.

The reaction orders of -0.29 and 1.07 for CO and O<sub>2</sub>, respectively, that were obtained in the absence of CO<sub>2</sub> were used for the determination of the reaction order with respect to CO<sub>2</sub>. The same computer program provided in POLYMATH (see Section 4.2.1.1) was used for the determination of rate expressions in the presence of CO<sub>2</sub>. As a result of these calculations, the reaction order with respect to the CO<sub>2</sub> partial pressure was found to be -1.31. The reaction rate constant ( $k'$ ) and the variance of the experimental error ( $\sigma^2$ ) were determined as 0.11 μmol.g<sup>-1</sup>.s<sup>-1</sup>.atm<sup>0.53</sup> and 0.013 (μmol.g<sup>-1</sup>.s<sup>-1</sup>)<sup>2</sup>, respectively.

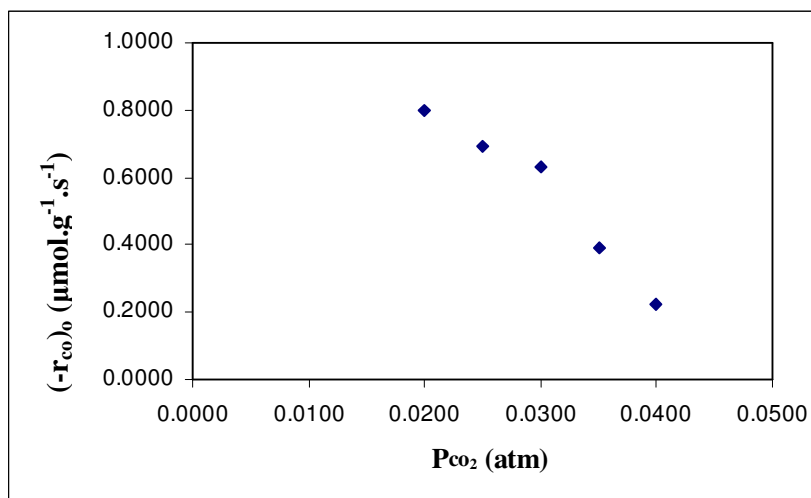


Figure 4.2. CO oxidation rate vs. CO<sub>2</sub> partial pressure over 1%Pt-1%CeO<sub>x</sub>/AC2 at 383 K using a feed composition of  $P_{CO} = 0.05$  atm and  $P_{O_2} = 0.025$  atm

The power-function rate expression for low-temperature CO oxidation at 383 K over 1%Pt-1%CeO<sub>x</sub>/AC2 in the presence of CO<sub>2</sub> can be stated as follows:

$$(-r_{CO})_o = 0.11(P_{CO})^{-0.29}(P_{O_2})^{1.07}(P_{CO_2})^{-1.31} \quad (4.8)$$

Langmuir-Hinshelwood expressions illustrated in Table 4.6 for the low-temperature oxidation of CO in the presence of CO<sub>2</sub> were also tested. Nonlinear regression with the Levenberg-Marquardt scheme provided in POLYMATH 5.1 were used for this purpose.

Table 4.6. Langmuir-Hinshelwood rate expressions tested for low-temperature CO oxidation in the presence of CO<sub>2</sub> at 383 K

Model No	Proposed Rate Equations	Rate Parameters	$\sigma^2$ ( $\mu\text{mol.g}^{-1}.\text{s}^{-1}$ ) <sup>2</sup>
1	$(-r_{co})_o = \frac{kP_{o_2}}{(1 + K_{co_2}P_{co_2})^2}$	$k = 102 \mu\text{mol.g}^{-1}.\text{s}^{-1}.\text{atm}^{-1}$ $K_{co_2} = 39.7 \text{ atm}^{-1}$	0.014
2	$(-r_{co})_o = \frac{kP_{o_2}}{(1 + K_{co_2}P_{co_2})}$	$k = 88 \mu\text{mol.g}^{-1}.\text{s}^{-1}.\text{atm}^{-1}$ $K_{co_2} = 102 \text{ atm}^{-1}$	0.024
3	$(-r_{co})_o = \frac{2kP_{o_2}}{(1 + K_{co}P_{co})(1 + K_{co_2}P_{co_2})^2}$	$k = 5.8 \mu\text{mol.g}^{-1}.\text{s}^{-1}.\text{atm}^{-1}$ $K_{co_2} = 26.9 \text{ atm}^{-1}$ $K_{co} = 102 \text{ atm}^{-1}$	0.028
4	$(-r_{co})_o = \frac{kK_{o_2}K_{co}P_{o_2}P_{co}}{(1 + K_{o_2}P_{o_2} + K_{co}P_{co} + K_{co_2}P_{co_2})^2}$	$k = 24.7 \mu\text{mol.g}^{-1}.\text{s}^{-1}$ $K_{o_2} = 32.6 \text{ atm}^{-1}$ $K_{co} = 17.6 \text{ atm}^{-1}$ $K_{co_2} = 101.9 \text{ atm}^{-1}$	0.042

Among these equations the first one seems to be the best. This rate equation is also agreement with the order of  $-1.31$  with respect to CO<sub>2</sub> and  $1.07$  with respect to O<sub>2</sub> obtained by using power-function rate expression. The variance of the experimental error also decreased with the addition of the CO<sub>2</sub>. The other Langmuir-Hinshelwood rate expressions also confirm these reaction orders.

#### 4.2.3. Effects of H<sub>2</sub> on Low-Temperature CO Oxidation

The effect of H<sub>2</sub> on the CO oxidation rate over 1%Pt-1%CeO<sub>x</sub>/AC2 was assessed by comparing with the kinetic data for CO oxidation in the absence of H<sub>2</sub>. Low-temperature CO oxidation was studied at 383 K in the presence of 5 per cent CO, 2.5 per cent O<sub>2</sub> and

different H<sub>2</sub> concentrations with balance He using 150 ml.min<sup>-1</sup> with a catalyst loading of 250 mg.

Table 4.7. CO and O<sub>2</sub> conversions for CO oxidation over 1%Pt-1%CeO<sub>x</sub>/AC2 at 383 K in the presence of H<sub>2</sub> and balance He

Exp. No	CO %	$F_{CO}$ (ml/min)	O <sub>2</sub> %	$F_{O_2}$ (ml/min)	H <sub>2</sub> %	$F_{H_2}$ (ml/min)	fractional conversions at 90 min TOS	
							$x_{CO}$	$x_{O_2}$
19	5	7.5	2.5	3.75	0	0	0.052	0.055
26	5	7.5	2.5	3.75	5	7.5	0.049	0.064
27	5	7.5	2.5	3.75	10	15	0.032	0.046
28	5	7.5	2.5	3.75	15	22.5	0.029	0.074
29	5	7.5	2.5	3.75	20	30	0.025	0.040
30	5	7.5	2.5	3.75	40	60	0.021	0.056
31	5	7.5	2.5	3.75	60	90	0.019	0.060

The addition of 5 per cent H<sub>2</sub> to the feed stream that contains 5 per cent CO, 2.5 per cent O<sub>2</sub> and balance He did not effect the CO oxidation activity very much; however, CO conversion declined considerably when the H<sub>2</sub> content was increased to 10 per cent which was followed by a small decrease that leveled out after 20 per cent H<sub>2</sub> addition. These results are presented in Table 4.7 and plotted in Figure 4.3.

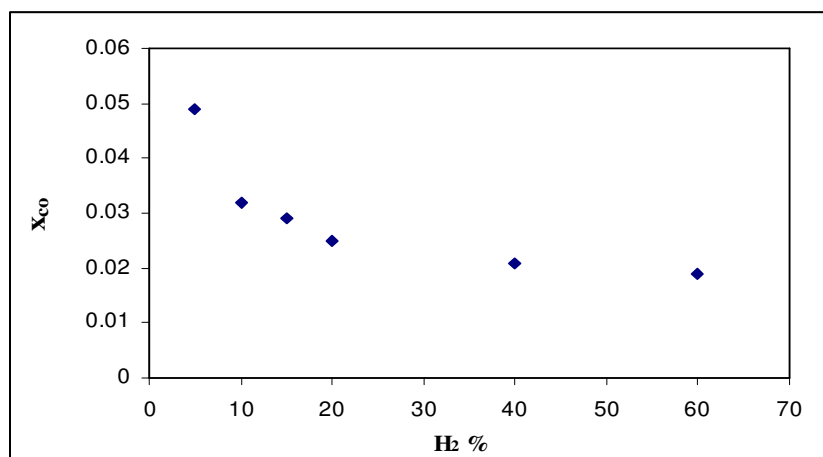


Figure 4.3. Effect of H<sub>2</sub> content on CO conversions over 1%Pt-1%CeO<sub>x</sub>/AC2 at 383 K

In order to remove CO completely from H<sub>2</sub>-rich gas in practice, O<sub>2</sub>/CO ratios greater than one have to be employed (Oh and Sinkevitch, 1993); however, this also leads to increased probability of H<sub>2</sub> oxidation which is undesirable. In this study, O<sub>2</sub>/CO ratio was kept constant at the stoichiometric ratio of 0.5 in preferential oxidation experiments. The presence of CO in stoichiometric amount may lead to blockage of active sites by CO which decreases the adsorption probability of O<sub>2</sub>. The effect of H<sub>2</sub> content in the feed on CO oxidation rates over 1%Pt-1%CeO<sub>x</sub>/AC2 at 383 K is presented in Figure 4.4 which shows that the CO oxidation rate is unaffected by increases in H<sub>2</sub> content above 20 volume per cent.

The present kinetic experiments show that CO oxidation would occur similarly in the presence of small amounts (ca.5 per cent) of H<sub>2</sub> as in the absence of hydrogen. Therefore, at low H<sub>2</sub> concentrations, a new rate expression is not necessary. Although the CO oxidation rate slows down with further addition of H<sub>2</sub>, CO oxidation rates obtained become nearly the same above 20 per cent. Preferential CO oxidation in H<sub>2</sub>-rich streams is a promising method for H<sub>2</sub> clean-up in fuel processor/fuel cell systems; and in PROX reactors, feeds with H<sub>2</sub> percentages between 45-60 per cent are involved. Since the hydrogen is in great excess, a H<sub>2</sub> dependence would not appear in the rate expression for CO oxidation; but it would be interesting to find out how the reaction orders with respect

to CO and O<sub>2</sub> are modified, if at all, by the presence of excess H<sub>2</sub>. These results may provide an insight on the role of different active sites in the CO oxidation mechanism.

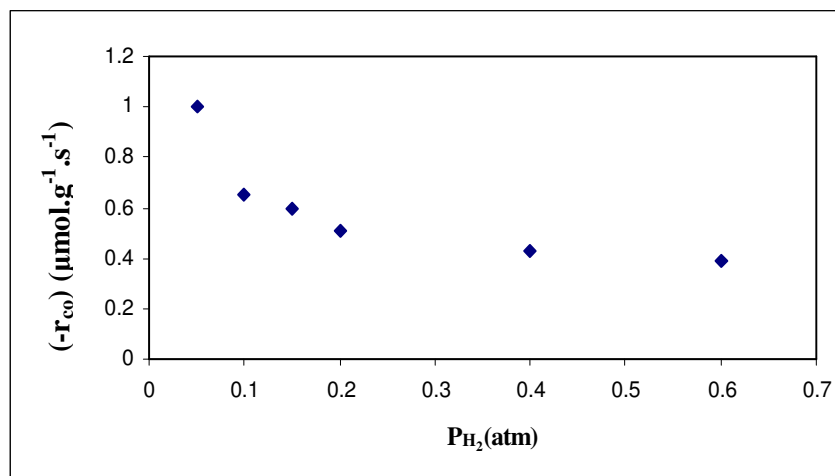


Figure 4.4. Effect of H<sub>2</sub> partial pressure on CO oxidation rates rate

In the presence of large quantities of hydrogen at 383 K, the conversion and reaction rate of CO may have decreased because of hydrogen oxidation. This would be consistent with the work of Pozdnyakova *et al.* (2006a) who studied PROX over the Pt/CeO<sub>x</sub> catalyst at low temperatures. They proposed that a low-temperature water-gas shift type reaction producing CO<sub>2</sub> and H<sub>2</sub> occurs at the Pt-ceria interface between linearly adsorbed CO molecules (on Pt) and adsorbed water (on ceria). A noncompetitive Langmuir-Hinshelwood mechanism has been described, involving CO activation on Pt particles and their reaction with oxygen activated from the support on the metal/oxide interface at low temperatures between 363-423 K (Pozdnyakova *et al.*, 2006b; Wootsch *et al.*, 2004). On the other hand, competitive hydrogen adsorption on Pt (and hence the possibility toward nonselective oxidation) is suppressed by the high (but not total) CO coverage, even in excess H<sub>2</sub>. The kinetic results of this study may even suggest that a noncompetitive Langmuir-Hinshelwood mechanism is also possible for the Pt-CeO<sub>x</sub>/AC2 catalyst.

One cause for the CO inhibition is the likely strong adsorption of CO on the Pt surfaces. Due to the high concentration of H<sub>2</sub> in the reactants, competing reactions ( $H_2 + \frac{1}{2} O_2 \rightarrow H_2O$ ) as well as H<sub>2</sub> adsorption on the surface may also occur. One possible mechanism

may be that CO strongly adsorbs onto a Pt site, then H<sub>2</sub> reacts with the adsorbed CO to form H<sub>2</sub>O, leaving behind carbon on the surface; O<sub>2</sub> may then react with that carbon to re-form adsorbed CO. Clearly, there is a competition between CO adsorption, H<sub>2</sub> reaction with adsorbed CO or O<sub>2</sub> or both and the ability for the O<sub>2</sub> to react with the carbon to form CO<sub>2</sub> and subsequently desorb to free the site for another reaction.

Kolb *et al.* (2007) proposed that in preferential oxidation reaction the catalyst surface is almost completely covered by carbon monoxide up to certain channel length (gas residence time), and then abruptly decreases, when no carbon monoxide is left in the gas phase. At the same time, the concentrations of adsorbed oxygen and hydrogen increases by almost an order of magnitude, which lead to a consumption of hydrogen due to water formation. The degree of water formation is merely limited by the amount of oxygen present in the gas phase. When all carbon monoxide and water are consumed, carbon monoxide is formed again via the reverse water-gas shift reaction.

## 5. CONCLUSIONS AND RECOMMENDATIONS

### 5.1. Conclusions

This work focuses on developing the kinetic expressions for low-temperature CO oxidation over air-oxidized activated carbon supported 1wt.%Pt-1wt.%CeO<sub>x</sub> catalyst prepared by sequential impregnation. Intrinsic kinetic data were obtained in the initial rates region at 383 K both in the absence of CO<sub>2</sub> or H<sub>2</sub> and in the presence of CO<sub>2</sub>. Preferential CO oxidation was also investigated in order to determine the effect of H<sub>2</sub> on CO oxidation rates using varying H<sub>2</sub> concentrations in the feed at constant residence time.

The major results obtained in this study can be summarized as follows:

- The kinetics of low-temperature CO oxidation within the parameter range investigated over Pt-CeO<sub>x</sub>/AC2 can be expressed by a simple power-law rate equation, with reaction orders of  $-0.29$  for CO and  $1.07$  for O<sub>2</sub>. These results indicate that oxygen may be adsorbed on the interfacial sites of Pt-CeO<sub>x</sub> while CO is adsorbed on the Pt surfaces of the catalyst. A negative order in CO and a positive order in O<sub>2</sub> close to unity indicate that the reaction rate controlled regime can be characterized for low-temperature CO oxidation.
- CO oxidation rates are found to decrease with increasing CO<sub>2</sub> content. The reaction order with respect to CO<sub>2</sub> in the power-function rate expression is calculated as  $-1.31$ .
- The reaction orders obtained with a power-law rate expression are consistent with the Langmuir-Hinshelwood reaction mechanism. No single rate expression describes the CO oxidation data; thus several plausible LHHW-type kinetic models are suggested for data obtained both in the absence and presence of CO<sub>2</sub>.
- Although CO oxidation rates are not significantly affected by H<sub>2</sub> concentrations below 5 per cent in the feed, a retarding effect is observed at higher H<sub>2</sub> concentrations which levels out above volume 20 per cent.

## 5.2. Recommendations

According to the results of the present study the following studies are recommended for kinetics of low-temperature CO oxidation both in the absence and presence of H<sub>2</sub>.

- Kinetic studies may be improved by performing several experiments at different temperatures to calculate the activation energy of the CO oxidation reaction, and hence, to obtain the effect of temperature on the mechanism over activated carbon supported Pt-CeO<sub>x</sub> catalyst.
- Kinetic experiments at various initial concentrations of CO and O<sub>2</sub> may be conducted in the presence of excess hydrogen ( $\geq 20$  volume per cent) to find out if the reaction orders with respect to CO and O<sub>2</sub> are changed and to gain further insight on how the AC surface may contribute to the catalytic reaction over Pt-CeO<sub>x</sub>.

## APPENDIX A: CONVERSION VERSUS RESIDENCE TIME GRAPHS

Carbon monoxide conversion versus residence time graphs for the low-temperature CO oxidation in the absence of both CO<sub>2</sub> and H<sub>2</sub> were illustrated as follows.

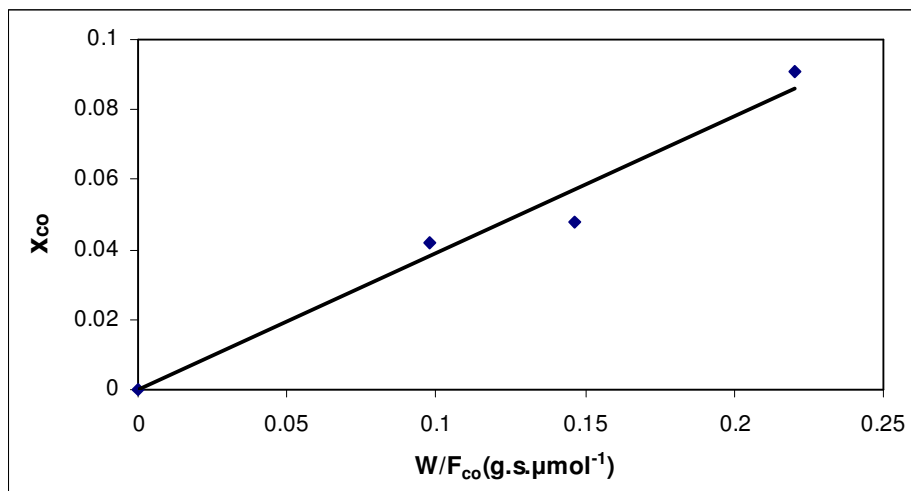


Figure A.1. Fractional CO conversion vs. residence time graph of experiments 1-3

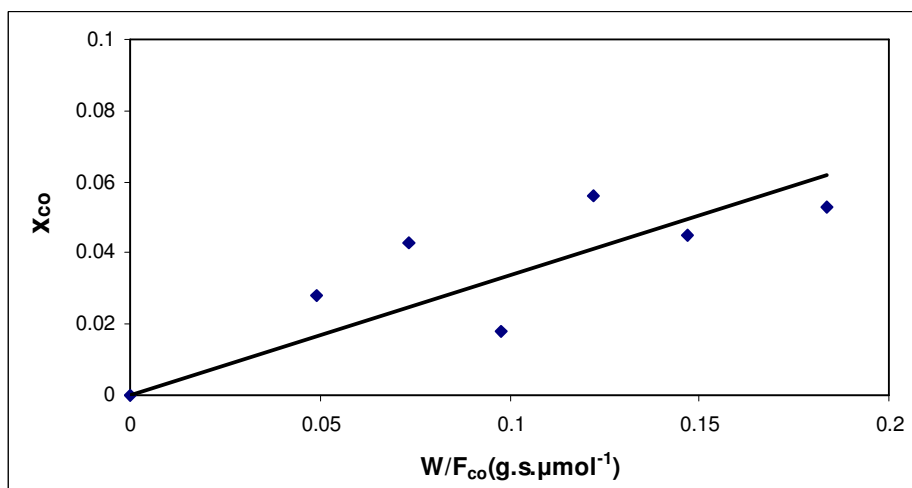


Figure A.2. Fractional CO conversion vs. residence time graph of experiments 4-9

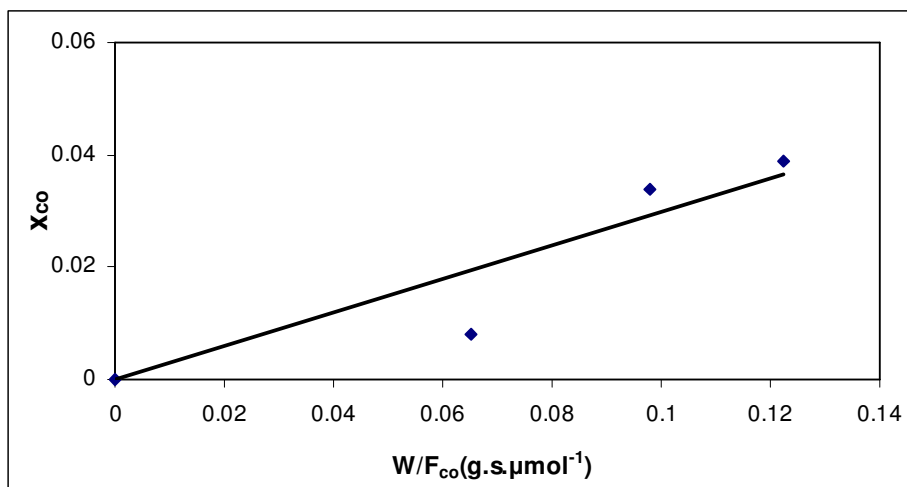


Figure A.3. Fractional CO conversion vs. residence time graph of experiments 10-12

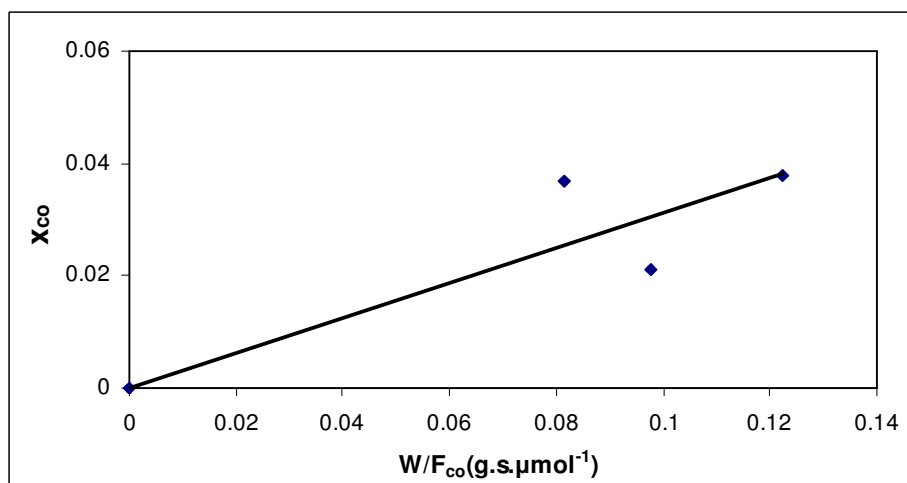


Figure A.4. Fractional CO conversion vs. residence time graph of experiments 13-15

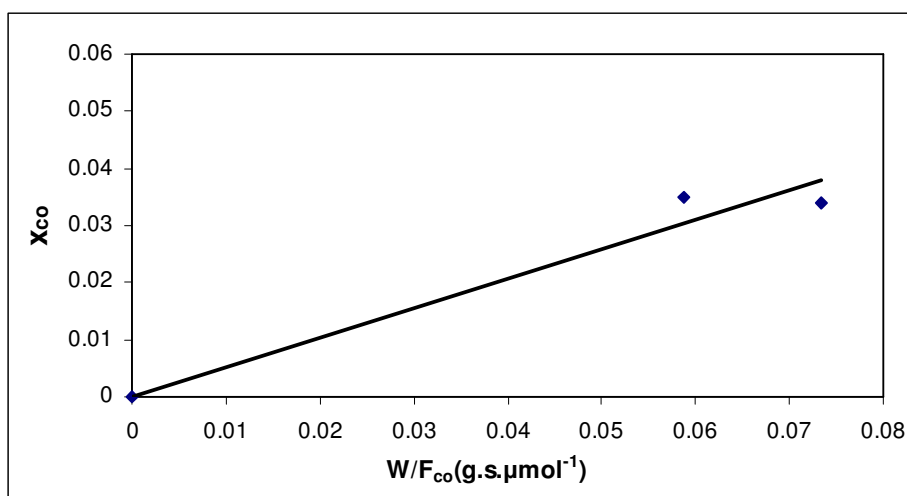


Figure A.5. Fractional CO conversion vs. residence time graph of experiments 17 and 18

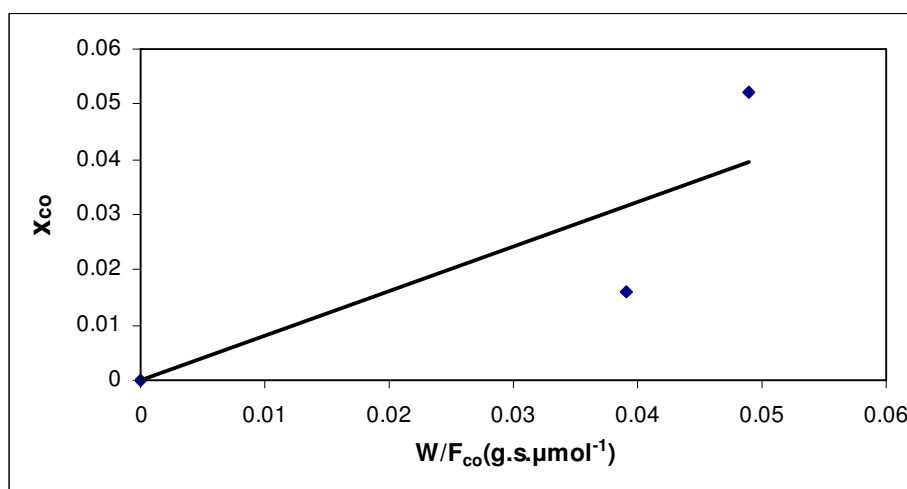


Figure A.6. Fractional CO conversion vs. residence time graph of experiments 19 and 20

Table A.1. The calculated rate data with using the fractional CO conversion vs. residence time graphs

Experiment No	Partial Pressures (atm)		$W_{cat} / F_{CO_{in}}$ (g.s. $\mu\text{mol}^{-1}$ )	$x_{CO}$	$(-r_{CO})_o$ ( $\mu\text{mol.g}^{-1}.\text{s}^{-1}$ )
	CO	O <sub>2</sub>			
1	0.01	0.01	0.220	0.091	0.3920
2			0.147	0.048	
3			0.098	0.042	
4	0.02	0.01	0.073	0.043	0.3368
5			0.049	0.028	
6			0.122	0.056	
7			0.098	0.018	
8			0.183	0.053	
9			0.147	0.045	
10	0.03	0.01	0.065	0.008	0.2995
11			0.122	0.039	
12			0.098	0.034	
13	0.03	0.015	0.082	0.037	0.3118
14			0.122	0.038	
15			0.098	0.021	
16	0.04	0.02	0.073	0.040	0.5452
17	0.05	0.02	0.073	0.034	0.5153
18			0.059	0.035	
19	0.05	0.025	0.049	0.052	0.8079
20			0.039	0.016	

## REFERENCES

- Akın, A. N., G. Kılaz, A. İ. İşli and Z. İ. Önsan, 2001, "Development and Characterization of Pt-SnO<sub>2</sub>/γ-Al<sub>2</sub>O<sub>3</sub> Catalysts", *Chemical Engineering Science*, Vol. 56, pp. 881-888.
- Aksoylu, A. E., M. Madalena, A. Freitas, J. L. Figueiredo, 2000a, "Bimetallic Pt-Sn Catalyst Supported on Activated Carbon I. The Effect of Support Modification and Impregnation Strategy", *Applied Catalysis A: General*, Vol.192, pp.29-42.
- Aksoylu, A. E., M. Madalena, A. Freitas, J. L. Figueiredo, 2000b, "Bimetallic Pt-Sn Catalyst Supported on Activated Carbon II. CO Oxidation", *Catalysis Today*, Vol.62, pp.337-346.
- Aksoylu, A. E., L. Faria, M.F.R. Pereira, J.L. Figueiredo, P. Serp, J.-C. Hierso, R. Feurer, Y. Kihn, P. Kalck, 2003, "Highly dispersed activated carbon supported platinum catalysts prepared by OMCVD: a comparison with wet impregnated catalysts", *Applied Catalysis A: General*, Vol.243, pp. 357-365.
- Aksoylu, A. E., M. Madalena, A. Freitas, M. Fernando, R. Pereira, J. L. Figueiredo, 2001, "The effects of different activated carbon supports and support modifications on the properties of Pt/AC catalysts", *Carbon*, Vol. 39, pp. 175–185.
- Alcaide F., P. Cabot, E. Brillas, 2006, "Fuel cells for chemicals and energy cogeneration", *Journal of Power Sources*, Vol.153, pp. 47-60.
- Anderson, J. R., M. Boudart, 1982, *Catalysis Science and Technology*, Springer-Verlag, Berlin Heidelberg, New York.
- Arias, A. M., A. B. Hungría, M. F. García, J. C. Conesa, G. Munuera, 2005, "Preferential Oxidation of CO in a H<sub>2</sub>-rich Stream Over CuO/CeO<sub>2</sub> and CuO/(Ce,M)O<sub>x</sub> (M = Zr, Tb) Catalysts", *Journal of Power Sources*, Vol. 151, pp. 32-42.

- Armor, J. N., 1992, "Environmental catalysis", *Applied Catalysis B: Environmental*, Vol. 1, pp. 221-256.
- Avgouropoulos, G., T. Ioannides, C. H. Papadopoulou, J. Batista, S. Hocevar and H. K. Matralis, 2002, "A Comparative Study of Pt/ $\gamma$ -Al<sub>2</sub>O<sub>3</sub>, Au/ $\alpha$ -Fe<sub>2</sub>O<sub>3</sub> and CuO-CeO<sub>2</sub> Catalysts for the Selective Oxidation of Carbon Monoxide in Excess Hydrogen", *Catalysis Today*, Vol. 75, pp. 157-167.
- Baschuk, J. J. and X. Li, 2001, "Carbon monoxide poisoning of proton exchange membrane fuel cells", *International Journal of Energy Research*, Vol. 25, pp. 695-713.
- Bencs, L., K. Ravindra, R. V. Grieken, 2003, "Methods for the determination of platinum group elements originating from the abrasion of automotive catalytic converters", *Spectrochimica Acta Part B*, Vol. 58, pp. 1723-1755.
- Boulahouache, A., G. Kons, H. G. Lintz, P. Schulz, 1992, "Oxidation of CO on platinum-tin dioxide catalysts at low temperatures", *Applied Catalysis A: General*, Vol. 91, pp. 115-123.
- Caputo, T., R. Pirone and G. Russo, 2006, "Supported CuO/Ce<sub>1-x</sub>Zr<sub>x</sub>O<sub>2</sub> catalysts for the preferential oxidation of CO in H<sub>2</sub>-rich gases", *Kinetic and Catalysis*, Vol. 47, pp. 756-764.
- Cheekatamarla, P., K. William, S. Epling and A. M. Lane, 2005, "Selective Low-Temperature Removal of Carbon Monoxide from Hydrogen-Rich Fuels over Cu-Ce-Al Catalysts", *Journal of Power Sources*, Vol. 147, pp. 178-183.
- Chen, L., D. Ma, B. Pietruszka, X. Bao, 2006, "Carbon-Supported Silver Catalysts for CO Selective Oxidation in Excess Hydrogen", *Journal of Natural Gas Chemistry*, Vol. 15, pp. 181-190.

- Choi, Y. and H. G. Stenger, 2004, “Kinetics, Simulation and Insights for CO Selective Oxidation in Fuel Cell Applications”, *Journal of Power Sources*, Vol. 129, pp. 246-254.
- Fogler, H. S., 1999, *Elements of Chemical Reaction Engineering*, Prentice-Hall, Englewood Cliffs, New Jersey.
- Fraga, M. A., E. Jordão, M. J. Mendes, M. M. A. Freitas, J. L. Faria, and J. L. Figueiredo, 2002, “Properties of Carbon-Supported Platinum Catalysts: Role of Carbon Surface Sites”, *Journal of Catalysis*, Vol. 209, pp. 355–364.
- Fuente, A. M., G. Pulgar, F. González, C. Pesquera, C. Blanco, 2001, “Activated carbon supported Pt catalysts: effect of support texture and metal precursor on activity of acetone hydrogenation”, *Applied Catalysis A: General*, Vol. 208, pp. 35–46.
- Ghenciu, A. F., 2002, “Review of fuel processing catalysts for hydrogen production in PEM fuel cell systems”, *Current Opinion in Solid State and Materials Science*, Vol. 66, pp. 389-399.
- Grass K. And H. G. Lintz, 1997, “The Kinetics of Carbon Monoxide Oxidation on Tin (IV) Oxide Supported Platinum Catalysts”, *Journal of Catalysis*, Vol. 172, pp. 446-452.
- Han, Y. F., M. Kinne, R.J. Behm, 2004, “Selective Oxidation of CO on Ru/ $\gamma$ -Al<sub>2</sub>O<sub>3</sub> in Methanol Reformate at Low Temperatures”, *Applied Catalysis B: Environmental*, Vol. 52, pp. 123-134.
- Herz, R. K., A. Badlani, D. R. Schryer, B. T. Upchurch, 1993, “Two-component catalysts for low-temperature CO oxidation: A Monte Carlo study”, *Journal of Catalysis*, Vol. 141, pp. 219-238.

- Igarashi, H., H. Uchida, M. Suzuki, Y. Sasaki and M. Watanabe, 1997, "Removal of Carbon Monoxide from Hydrogen-Rich Fuels by Selective Oxidation over Platinum Catalyst Supported on Zeolite", *Applied Catalysis A: General*, Vol. 159, pp. 159-169.
- Kahlich, M., J. H. A. Gasteiger and R. J. Behm, 1997, "Kinetics of the Selective CO Oxidation in H<sub>2</sub>-Rich Gas on Pt/Al<sub>2</sub>O<sub>3</sub>", *Journal of Catalysis*, Vol. 171, pp. 93-105.
- Kim, D. H. and M. S. Lim, 2002, "Kinetics of Selective CO Oxidation in Hydrogen-Rich Mixtures on Pt/Alumina Catalysts", *Applied Catalysis A: General*, Vol. 224, pp. 27-38.
- Kielin, E. J., 1998, *Platinized tin oxide: a low-temperature oxidation catalyst*, Ph.D. Thesis, College of William & Mary.
- Kolb, G., V. Hessel, V. Cominos, C. Hofmann, H. Löwe, G. Nikolaidis, R. Zapf, A. Ziogas, E.R. Delsman, M.H.J.M. de Croon, J.C. Schouten, O. de la Iglesia, R. Mallada, J. Santamaria, 2007, "Selective Oxidations in Micro-Structured Catalytic Reactors-For Gas-Phase Reactions and Specifically for Fuel Processing for Fuel Cells", *Catalysis Today*, Vol. 120, pp. 2-20.
- Korotkikh, O. and R. Farrauto, 2000, "Selective Catalytic Oxidation of CO in H<sub>2</sub>: Fuel Cell Applications", *Catalysis Today*, Vol. 62, pp. 249-254.
- Luengnaruemitchai, A., S. Osuwan and E. Gulari, 2004, "Selective catalytic oxidation of CO in the presence of H<sub>2</sub> over gold catalyst", *International Journal of Hydrogen Energy*, Vol. 29, pp. 215-221.
- Manasilp, A. and E. Gulari, 2002, "Selective CO oxidation over Pt/alumina catalysts for fuel cell applications", *Applied Catalysis B: Environmental*, Vol. 37, pp. 17-25.

- Mariño, F., C. Descorme and D. Duprez, 2004, “Noble Metal Catalysts for the Preferential Oxidation of Carbon Monoxide in the Presence of Hydrogen (PROX)”, *Applied Catalysis B: Environmental*, Vol. 54, pp. 59-66.
- Maunula, T., J. Ahola, T. Salmi, H. Haario, M. Häkönen, M. Luoma, V. J. Pohjola, 1997, “Investigation of CO oxidation and NO reduction on three-way monolith catalysts with transient response techniques”, *Applied Catalysis B: Environmental*, Vol. 12, pp. 287-308.
- Masel, R. I., 2001, *Chemical Kinetics and Catalysis*, Wiley-Interscience, New York.
- Maruyama, J. and I. Abe, 2005, “Enhancement effect of an adsorbed organic acid on oxygen reduction at various types of activated carbon loaded with platinum”, *Journal of Power Sources*, Vol. 148, pp. 1–8.
- Min, M., C. Park, H. Kim, C. Kwak, A. A. Serov, H. Kweon, S. Lee, 2006, “Nano-fabrication and characterization of new conceptual platinum catalysts for low temperature fuel cells”, *Electrochimica Acta*, Vol. 52, pp.1670-1675.
- Minh, C. L. and T. C. Brown, 2006, “Rate parameters from low-pressure steady-state protolytic cracking and dehydrogenation of isobutane over zeolite catalysts”, *Applied Catalysis A: General*, Vol. 310, pp. 145–154.
- Nibbelke, R. H., M. A. J. Campman, J. H. B. J. Hoebink and G. B. Marin, 1997, “Kinetic Study of the CO Oxidation over Pt/ $\gamma$ -Al<sub>2</sub>O<sub>3</sub> and Pt/Rh/CeO<sub>2</sub>/ $\gamma$ -Al<sub>2</sub>O<sub>3</sub> in the Presence of H<sub>2</sub>O and CO<sub>2</sub>”, *Journal of Catalysis*, Vol. 171, pp. 358-373.
- Nibbelke, R. H., A. J. L. Nievergeld, J. H. B. J. Hoebink and G. B. Marin, 1998, “Development of a Transient Kinetic Model for the CO Oxidation by O<sub>2</sub> over a Pt/Rh/CeO<sub>2</sub>/ $\gamma$ -Al<sub>2</sub>O<sub>3</sub> Three-Way Catalyst”, *Applied Catalysis B: Environmental*, Vol. 19, pp. 245-259.

- Oh, S. H. and G. B. Hoflund, 2007, "Low-temperature catalytic carbon monoxide oxidation over hydrous and anhydrous palladium oxide powders", *Journal of Catalysis*, Vol. 245, pp. 35–44.
- Oh, S.H. and Sinkevitch, R. M., 1993, "Carbon Monoxide Removal from Hydrogen-Rich Fuel Cell Feed streams by Selective Catalytic Oxidation", *Journal of Catalysis*, Vol. 142, pp. 254-262.
- Oran, U. and D. Uner, 2004, "Mechanisms of CO Oxidation Reaction and Effect of Chlorine Ions on the CO Oxidation Reaction over Pt/CeO<sub>2</sub> and Pt/CeO<sub>2</sub>/γ-Al<sub>2</sub>O<sub>3</sub> catalysts", *Applied Catalysis B: Environmental*, Vol. 54, pp. 183-191.
- Ouyang, X. and R. S.Besser, 2005, "Effect of reactor heat transfer limitations on CO preferential oxidation", *Journal of Power Sources*, Vol. 141, pp. 39-46.
- Özkara, Ş., 2002, *Selective Low Temperature Carbon Monoxide Oxidation in H<sub>2</sub>-Rich Gas Streams over Zeolite and Activated Carbon Supported Catalysts*, M. S. Thesis, Boğaziçi University.
- Özkara, Ş. and A. E. Aksoylu, 2003, "Selective Low Temperature Carbon Monoxide Oxidation in H<sub>2</sub>-Rich Gas Streams over Activated Carbon Supported Catalysts", *Applied Catalysis A: General*, Vol. 251, pp. 75-83.
- Özyönüm, G. N., 2005, *Kinetics of Selective CO Oxidation in Hydrogen-Rich Streams Over Pt-Co-Ce/Al<sub>2</sub>O<sub>3</sub> Catalyst*, M. S. Thesis, Boğaziçi University.
- Pozdnyakova, O., D. Teschner, A. Wootsch, J. Kröhnert, B. Steinhauer, H. Sauer, L. Toth, F. C. Jentoft, A. Knop-Gericke, Z. Paál, R. Schlög, 2006a, "Preferential CO oxidation in hydrogen (PROX) on ceria-supported catalysts, part I: Oxidation state and surface species on Pt/CeO<sub>2</sub> under reaction conditions", *Journal of Catalysis*, Vol.237, pp.1-16.

- Pozdnyakova, O., D. Teschner, A. Wootsch, J. Kröhnert, B. Steinhauer, H. Sauer, L. Toth, F. C. Jentoft, A. Knop-Gericke, Z. Paál, R. Schlög, 2006b, "Preferential CO oxidation in hydrogen (PROX) on ceria-supported catalysts, part II: Oxidation state and surface species on Pd/CeO<sub>2</sub> under reaction conditions", *Journal of Catalysis*, Vol.237, pp.17-28.
- Rajasree, R., J. H. B. J. Hoebink and J. C. Schouten, 2004, "Transient Kinetics of Carbon Monoxide Oxidation by Oxygen over Supported Palladium/Ceria/Zirconia Three-Way Catalysts in the Absence and Presence of Water and Carbon Dioxide", *Journal of Catalysis*, Vol. 223, pp. 36-43.
- Ren, S. and X. Hong, 2006, "CO selective oxidation in hydrogen-rich gas over platinum catalysts", *Fuel Processing Technology*, Article in Press.
- Roberts, G. W., P. Chin, X. Sun, J. J. Spivey, 2003, "Preferential oxidation of carbon monoxide with Pt/Fe monolithic catalysts: interactions between external transport and the reverse water-gas-shift reaction", *Applied Catalysis B: Environmental*, Vol. 46, pp. 601-611.
- Rodriguez-Reinoso, F., 1998, "The Role of Carbon Materials in Heterogeneous Catalysis", *Carbon*, Vol.36, pp.159-175.
- Salomons, S., R. E. Hayes, M. Votsmeier, A. Drochner, H. Vogel, S. Malmberg, J. Gieshoff, 2007, "On the use of mechanistic CO oxidation models with a platinum monolith catalyst", *Applied Catalysis B: Environmental*, Vol. 70, pp. 305-313.
- Satterfield, C. N., 1991, *Heterogeneous Catalysis in Industrial Practice*, McGraw-Hill, USA.
- Schmal, M., M. M. V. M. Souza, N. S. Resende, A. L. Guimarães, C. A. Perez, J. G. Eon, D. A. G. Aranda and L. C. Dieguez, 2005, "Interpretation of Kinetic Data with Selected Characterizations of Active Sites", *Catalysis Today*, Vol. 100, pp. 145-150.

- Sedmak, G., S. Hocevar and J. Levec, 2004, "Transient Kinetic Model of CO Oxidation over a Nanostructured  $\text{Cu}_{0.1}\text{Ce}_{0.9}\text{O}_2$ -Catalyst", *Journal of Catalysis*, Vol. 222, pp. 87-99.
- Serre, C., F. Garin, G. Belot and G. Maire, 1993, "Reactivity of Pt/ $\text{Al}_2\text{O}_3$  and Pt-CeO<sub>2</sub>/ $\text{Al}_2\text{O}_3$  Catalysts for the Oxidation of Carbon Monoxide by Oxygen II. Influence of the Pretreatment Step on the Oxidation Mechanism", *Journal of Catalysis*, Vol. 141, pp. 9-20.
- Shalabi, M. A., B. H. Harji, C. N. Kenney, 1996, "Kinetic Modelling of CO Oxidation on Pt/CeO<sub>2</sub> in a Gradientless Reactor", *Journal of Chemical Technology and Biotechnology*, Vol. 65, pp. 317-324.
- Son, I. H., M. Shamsuzzoha and A. M. Lane, 2002, "Promotion of Pt/ $\gamma$ - $\text{Al}_2\text{O}_3$  by New Pretreatment for Low-Temperature Preferential Oxidation of CO in H<sub>2</sub> for PEM Fuel Cells", Research Note, *Journal of Catalysis*, Vol. 210, pp. 460-465.
- Son, I. H., 2006, "Study of Ce-Pt/  $\gamma$  - $\text{Al}_2\text{O}_3$  for the selective oxidation of CO in H<sub>2</sub> for application to PEFCs: Effect of gases", *Journal of Power Sources*, Vol. 159, pp. 1266-1273.
- Souza, M. V. M. M., N. F.P. Ribeiro, M. Schmal, 2006, "Influence of the support in selective CO oxidation on Pt catalysts for fuel cell applications", *International Journal of Hydrogen Energy*, Article in Press.
- Stefanov P. K., Y. Ohno, T. Yamanaka, Y. Seimiya, K. Kimura, T. Matsushima, 1998, "Reaction dynamics of catalytic CO oxidation on a Pt(113) surface", *Surface Science*, Vol. 416, pp. 305-319.
- Şimşek, E., 2005, "Preferential CO Oxidation Over Activated Carbon Supported Noble Metal Reducible Oxide Catalysts", M. S. Thesis, Boğaziçi University.

- Şimşek, E., Ş. Özkara, A. E. Aksoylu, Z. İ. Önsan, 2007, "Preferential CO oxidation over activated carbon supported catalysts in H<sub>2</sub>-rich gas streams containing CO<sub>2</sub> and H<sub>2</sub>O", *Applied Catalysis A: General*, Vol. 316, pp. 169–174.
- Teschner, D., A. Wootsch, O. Pozdnyakova, H. Sauer, A. Knop-Gericke, R. Schlögl, 2006, "Surface and Structural Properties of Pt/CeO<sub>2</sub> Catalyst Under Preferential CO Oxidation in Hydrogen (PROX)", *Reaction Kinetics and Catalysis Letter*, Vol. 87, pp. 235-247.
- Tibiletti, D., E. A. B. Graff, S. P. Teh, G. Rothenberg, D. Farrusseng, C. Mirodatos, 2004, "Selective CO Oxidation in the Presence of Hydrogen: Fast Parallel Screening and Mechanistic Studies on Ceria-Based Catalysts", *Journal of Catalysis*, Vol. 225, pp. 489-497.
- Trimm, D. L. and Z. İ. Önsan, 2001, "Onboard Fuel Conversion for Hydrogen-Fuel-Cell-Driven Vehicles", *Catalysis Reviews-Science and Engineering*, Vol. 43 (1-2), pp. 31-84.
- Trimm, D. L., 2005, "Minimisation of Carbon Monoxide in a Hydrogen Stream for Fuel Cell Application", *Applied Catalysis A: General*, Vol. 296, pp. 1-11.
- Vanderbosch, R. H., W. Prins, W. P. M. van Swaaij, 1998, "Platinum Catalyzed Oxidation of Carbon Monoxide as a Model Reaction in Mass Transfer Measurements", *Chemical Engineering Science*, Vol. 53, pp. 3355-3366.
- Wang, B., 2005, "Recent Development of Non-platinum Catalysts for Oxygen Reduction reaction", *Journal of Power Sources*, Vol.152, pp. 1–15.
- Wee, J. H. and K. Y. Lee, 2006, "Overview of the Development of CO-tolerant Anode Electrocatalysts for Proton-Exchange Membrane Fuel Cells", *Journal of Power Sources*, Vol. 157, pp. 128-135.

- Wootsch, A., C. Descorme and D. Duprez, 2004, "Preferential Oxidation of Carbon Monoxide in the Presence of Hydrogen (PROX) over Ceria–Zirconia and Alumina-Supported Pt Catalysts", *Journal of Catalysis*, Vol. 225, pp. 259-266.
- Zafiridis, G. S. and R. J. Gorte, 1993, "CO Oxidation on Pt/ $\alpha$ -Al<sub>2</sub>O<sub>3</sub> (0001): Evidence for Structure Sensitivity", *Journal of Catalysis*, Vol. 140, pp. 418-423.
- Zhdanov, V. P. and B. Kasemo, 2003, "The Effect of Oxide Formation on Bistability in CO Oxidation on Pt", *Journal of Catalysis*, Vol. 220, pp. 478-485.
- Zhu, H., Z. Qin, W. Shan, W. Shen, J. Wang, 2005, "Low-Temperature Oxidation of CO Over Pd/CeO<sub>2</sub>–TiO<sub>2</sub> Catalysts with Different Pretreatments", *Journal of Catalysis*, Vol. 233, pp. 41–50.